Enhanced FcγRIII/CD16 activation by discrete ligands as independent correlates of disease severity in COVID-19 patients

Jakob Ankerhold[1,2,11] & Sebastian Giese[1,2,11] & Philipp Kolb[1,2,11], Andrea Maul-Pavicic[3,4], Nathalie Göppert[1,2], Kevin Ciminski[1,2], Clemens Kreutz[5], Achim Lother[6,7], Ulrich Salzer[3], Wolfgang Bildl[8], Tim Welsink[9], Nils G. Morgenthaler[9], Andrea Busse Grawitz[10], Daniela Huzly[1,2], Martin Schwemmle[1,2], Hartmut Hengel[1,2,12], Valeria Falcone[1,2,12]

[1]Institute of Virology, University Medical Center, Albert-Ludwigs-University Freiburg, Hermann-Herder-Str. 11, 79104 Freiburg, Germany
[2]Faculty of Medicine, Albert-Ludwigs-University Freiburg, 79104 Freiburg, Germany
[3]Department of Rheumatology and Clinical Immunology, Medical Center-University of Freiburg, Faculty of Medicine, University of Freiburg, Hugstetterstr. 55, 79106 Freiburg, Germany
[4]Center for Chronic Immunodeficiency (CCI), Medical Center-University of Freiburg, Faculty of Medicine, University of Freiburg, Breisacherstr. 115, 79106 Freiburg, Germany
[5]Institute of Medical Biometry and Statistics, Faculty of Medicine and Medical Center, University of Freiburg, Stefan Meier Str. 26, 79104 Freiburg, Germany
[6]Heart Center Freiburg University, Department of Cardiology and Angiology I, Faculty of Medicine, University of Freiburg, Hugstetterstr. 55, 79106 Freiburg, Germany
[7]Institute of Experimental and Clinical Pharmacology and Toxicology, Faculty of Medicine, University of Freiburg, Albertstr. 25, 79104 Freiburg, Germany
[8]Institute of Physiology II, Faculty of Medicine, University of Freiburg, Hermann-Herder-Str. Freiburg, Germany
[9]InVivo BioTech Services GmbH, 16761 Hennigsdorf, Germany
[10]Institute of Clinical Chemistry and Laboratory Medicine, Medical Center - University of Freiburg, Faculty of Medicine, University of Freiburg, Hugstetterstr. 55, 79106 Freiburg, Germany
[11]contributed equally
[12]corresponding authors

One sentence summary

Severity of disease in COVID-19 patients is associated with enhanced CD16 activation by afucosylated S-specific IgG and CD16-reactive circulating IgG-complexes.

Abstract

A dysregulated immune response with high levels of SARS-CoV-2 specific IgG antibodies is a common and distinctive feature of severe or critical COVID-19. Although a robust IgG response is typically considered to be beneficial, an overshooting activation mediated by immune receptors recognizing the Fc part of IgG (FcγRs) is thought to be detrimental and associated with immunopathology. However, direct evidence of FcγR driven immunopathology in COVID-19 is still sparse. Here, we used a cell-based FcγR activation reporter system to systematically analyze SARS-CoV-2 specific IgG responses and IgG-mediated FcγRIII (CD16) activation profiles in COVID-19 patient cohorts categorized by severity of disease. We found that increased CD16 activation by SARS-CoV-2 specific IgG is associated with a known pro-inflammatory IgG modification, namely afucosylation. Further, we identified CD16-reactive soluble IgG immune complexes (sICs) to be present in the serum of COVID-19 patients and show that the resulting CD16 activation by sICs is strongly related to disease severity. Our results provide evidence that CD16 activation by pro-inflammatory SARS-CoV-2 specific IgG together with circulating sICs is a major contributor to COVID-19 immunopathology. These findings highlight the importance of FcγR driven immunopathology in COVID-19. Further, our data highly warrant the development of targeted intervention strategies against IgG driven immunopathology following SARS-CoV-2 infection.

Introduction

Since the emergence of SARS-CoV-2 in late December 2019[1], more than 178 million laboratory confirmed infections (as of June 21, 2021) have been reported, with cases continuously rising[2]. Accordingly, rapid insights into the disease manifestations and pathogenesis have been globally obtained. A hallmark of the coronavirus disease 2019 (COVID-19) is a respiratory infection which can progress to an acute respiratory distress syndrome (ARDS). Next to asymptomatic infections, COVID-19 symptoms differ widely according to the disease process and may comprise fever, coughing, pneumonia, dyspnea, hypoxia and lymphopenia[3]. While fever and coughing are common symptoms, pneumonia, hypoxia, dyspnea, certain organ manifestations and lymphopenia indicate critical or fatal infections. Pronounced dyspnea can eventually progress to ARDS, a severe complication frequently observed in critically ill patients[4]. Although disease severity and in particular breathing difficulties are related to viral load[5], age[6-8] and underlying medical conditions[7,8], the kinetics of respiratory failure strongly suggest an essential role of the host immune response[3,7]. Typically, aggravation occurs between 9-12 days after symptom onset[8] and correlates with high levels of SARS-CoV-2 specific IgG antibodies and systemic effects of pro-inflammatory cytokines such as IL-6 and TNFα[3,9,10]. This cytokine release, primarily the result of macrophage and T helper (T_H) cell activation[11], includes pattern recognition receptor (PRR) signaling in the context of innate immunity but also Fcγ receptor (FcγR) activation[12]. Triggered by immune complexes (antibody-antigen complex), the cytokine release following FcγR activation represents a potent defense mechanism against invading pathogens. A prototypical activating FcγR in this regard is FcγRIII (CD16) expressed by NK cells and monocyte-derived macrophages (CD16A)[13] or neutrophils (CD16B, 98% sequence identical ectodomains). Specifically, CD16 is able to recognize circulating soluble immune complexes (sICs) as they are formed in certain autoimmune diseases such as lupus[14-17] and viral infections[18]. Overstimulation of activating FcγRs in these cases is associated with disease severity[18-20] and thus an FcγR-driven overshooting inflammatory response[12] might be an explanation for the pronounced immunopathology observed during severe courses of COVID-19[21]. Consistently, hyper-inflammation in SARS-CoV-1 and MERS infected patients has been previously proposed as a possible pathogenic factor[22] and could be demonstrated in mice and macaques infected with SARS-CoV-1[23,24]. Furthermore, N297-dependent glycan-modifications such as afucosylation within the constant region of SARS-CoV-2 specific IgG antibodies enhance binding to FcγRs, in turn driving inflammation. Enhanced FcγR activation

by low-fucosylated anti-SARS-CoV-2-S IgG leading to excessive alveolar macrophage activation has specifically been shown to drive severe COVID-19 disease progression[25].

Therefore we aimed to delineate the contribution of IgG-mediated effector functions regarding COVID-19 severity in patient cohorts with various severity of SARS-CoV-2 infection. We monitored antigen-specific IgG responses in patients with mild, critical and severe COVID-19 disease with regard to titer, kinetics and CD16 activation. This revealed a marked correlation between CD16 activation by patient IgG and severity of disease. Additionally, we identified circulating sICs to be abundantly present in the serum of critically and severely diseased patients, but not in the serum of those with a mild disease. As sIC-mediated CD16 activation independently correlates with disease severity, we provide evidence that also sIC formation is indicative of disease progression. Our findings enable new avenues of intervention against COVID-19 and highly warrant further investigation into the origin and composition of sICs in COVID-19.

Results

Patients and clinical information.

We retrospectively analyzed serial serum samples collected for routine diagnostic testing from 41 patients hospitalized at our tertiary care center between March and June 2020 with SARS-CoV-2 infection confirmed by real-time PCR. Based on the clinical course, we categorized patients as either severely diseased (hospitalized with COVID-19 related pneumonia) versus critically diseased (COVID-19 related pneumonia and eventually in need of invasive mechanical ventilation). In total, 27 patients with critical and 14 with severe courses of disease were grouped into separate cohorts (Table 1). Most patients were older than 60 years with an overall mean age of 68 years (63 years and 76 years in the critically and severely diseased patients respectively).

The majority of patients in both groups had comorbidities of different origin with cardiovascular diseases including hypertension representing the most frequent pathology (35/41, 85%). Similar to previous reports, high Interleukin 6 (IL-6) and C-reactive protein (CRP) levels were associated with severity of disease (Ø IL-6: 1452.1 pg/ml in the critical group vs 46.1 pg/ml in the severe group and Ø CRP: 162.2 mg/l vs 65.3 mg/l Ø13-25 days post symptom onset respectively). Similarly, procalcitonin, a biomarker of microbial coinfection, was significantly higher in critically diseased patients (Ø value 9.9 ng/ml vs 0.17 ng/ml). Bacterial superinfection represented a further complication in 39% of the patients and

was only slightly more frequent in patients with critical disease (11/27, 41% vs 5/14, 33%). More than half of the patients (59%) were treated with hydroxycloroquine/Kaletra®, (18/27, 67% in the critical group vs 6/14, 43% in the severe group). Notably, at the time of serum acquisition, only one patient received steroid treatment, which was given due to underlying chronic obstructive pulmonary disease. Finally, mortality rate was 37% (10/27) in critically and 7% (1/14) in severely diseased patients.

Kinetics of IgG antibody responses following symptom onset across severe and critical courses of disease.

It has been proposed that elevated SARS-CoV-2 antibody titers are associated with disease severity[10] and may play a role not only in the clearance but also in the pathogenesis of SARS-CoV-2 infection[26]. We therefore initially analyzed the levels and kinetics of SARS-CoV-2 specific IgG in serial serum samples from patients hospitalized with critical (n=27) or severe (n=14) illness, a setting we also used in the following experiments. A total of 125 (critically diseased) and 79 (severely diseased) serum samples, obtained from the aforementioned patients at different time points within 6-25 days following symptom onset were analyzed by commercially available S1- and N- specific ELISA-based assays. Assay specificity was confirmed analyzing healthy donor (HD) serum samples (n=30) as negative control (Figure 1-figure supplement 1 A, B). Most patients developed detectable SARS-CoV-2 specific IgG responses within 9-14 days after symptom onset. SARS-CoV-2 specific IgG gradually increased over time in both severely and critically diseased patients reaching a plateau at 18-20 days after symptom onset (Figure 1 A, B). Varying antibody response kinetics were observed for each individual patient (Figure 1-figure supplement 2 A-D) with anti-N IgG titers rising significantly earlier than anti-S1 IgG (12.5 days ± 3.3 days vs 10.6 ± 3.8; p= 0.0091). A trend towards earlier seroconversion for anti-S1 IgG could be observed in critically diseased patients (mean time of seroconversion 11.4 ± 3.0 days in critically diseased patients vs 12.9 ± 3.8 days for severely diseased patients; p = 0.24), whereas time of seroconversion for anti-N IgG was similar in both groups (10.1 ± 3.2 and 10.4 ± 4.2 days for critically and severely diseased patients, respectively; p = 0.83). S1- and N-specific IgG levels at plateau did not significantly differ between the two groups. No significant difference between deceased and discharged patients was measured 13-25 days after symptom onset (Figure 1- figure supplement 1 C, D, E). Next, we evaluated and compared the neutralizing capacity of SARS-CoV-2 IgG in either critically versus severely diseased patients in a plaque-reduction assay (Figure 1 C). All patients mounted a robust neutralizing antibody response

(91% ± 10.5 % neutralization at a 1:64 serum dilution), with peaking titers at 18-20 days following symptom onset. Of note, two critically diseased patients developed a neutralizing response already at 6-8 days after symptom onset. In summary, we observed only minor differences in cohort wide kinetics of S1- or N- specific IgG levels between patients hospitalized with severe or critical clinical courses indicating that antibody levels per se did not correlate with severity of disease in our study.

Patients with severe COVID 19 show enhanced CD16 activation by S-specific IgG antibodies.

FcγRIII (CD16) activation initiates multiple protective effector functions such as antibody-dependent cellular cytotoxicity (ADCC) by natural killer (NK) cells as well as antibody-dependent cytokine and chemokine secretion by NK cells and macrophages[12,27]. However, excessive FcγR stimulation can have severe adverse effects such as elevated cytokine release as observed in autoimmune diseases or viral infections[12]. Therefore, we hypothesized that an exaggerated FcγR mediated activation triggered by SARS-CoV-2 specific IgG might contribute to the exacerbation of COVID-19 in severely compared to critically diseased patients. To address this, we analyzed the ability of SARS-CoV-2 specific antibodies to activate CD16 (158V) using a previously established cell-based reporter system[28] (Figure 2-figure supplement 1A). Considering the typically late time point of health deterioration, we performed an analysis of CD16 activation triggered by SARS-CoV-2 specific IgG on serum samples obtained 13-25 days following symptom onset (Figure 2). Sera were analyzed at a 1:500 dilution to stay within the dynamic range of detection (Figure 2- figure supplement 2). Depending on the availability of sample material 2-8 samples/patient/time-point were included in this analysis. If available in sufficient quantity, sera were reanalyzed. Reproducibility was tested using available serum surplus (Figure 2- figure supplement 3). Sera from 28 patients with mild SARS-CoV-2 infection and 30 healthy blood donors were included for reference. Semi-quantitative assessment of IgG titers using antigen-specific ELISA revealed comparable levels between critically and severely diseased patient cohorts (Figure 2 A, B, C). In contrast, S- ($p=0.0147$) and RBD-specific ($p=0.0120$) but not N-specific IgG-mediated CD16 activation was significantly increased in critically compared to severely diseased patients (Figure 2 D-F). Furthermore, normalizing CD16 activation to antigen-specific IgG titers, revealed significantly stronger CD16 activation by S- ($p=0.0033$) and N-specific ($p=0.006$) IgG compared to mildly diseased patients (Figure 2 G-I). Intriguingly, we observed a heterogeneous CD16 activation pattern characterized by either

high or low CD16-activating sera irrespective of the clinical manifestation (Figure 2 D-F). Overall, a significant positive correlation could be determined between anti-SARS-CoV-2 antigen IgG titers and CD16 activation (Figure 2-figure supplement 4). Our data document a sustained CD16 activation by SARS-CoV-2 specific antibodies particularly in patients suffering from critical COVID-19 disease. Based on these results we confirmed the notion that elevated FcγRIII activation by S- and or RBD-specific IgG might contribute to disease severity of COVID-19.

Enhanced Fcγ-afucosylation of S-specific IgG in critically and severely diseased patients results in increased CD16 activation.

We speculated that differences in Fcγ mediated effector functions might contribute to disease severity of COVID-19 and thus compared CD16 high- versus CD16 low-activating patient sera regarding their SARS-CoV-2 specific IgG core fucosylation. Inspired by previous findings[29-31] we focused on determining IgG core fucosylation of S- and N- specific SARS-CoV2 IgG. To determine IgG core fucosylation we adapted a lectin-based ELISA preceded by antigen-specific antibody purification from immobilized SARS-CoV-2-antigen. Analysis of anti-S and anti-N IgG core fucosylation was performed on serum pools containing five sera of either critically or severely diseased patients obtained 13-25 days post symptom onset. Given the aforementioned heterogeneity in CD16-activation, we analyzed pools of 5 sera of either critically or severely diseased patients characterized by either high or low CD16-activation.To stay within the dynamic detection range, relative fucosylation was analyzed at a dilution of 1:4 (Figure 3). When analyzing serum pools from critically and severely diseased patients we determined a significantly lower level of core fucosylation among the high CD16 activators (Figure 3, plain-colored bars) compared to the low CD16 activators (Figure 3, shaded bars). This applied for both the S- and N-specific antibodies. These results are in line with previously published findings regarding the effect of Fcγ-afucosylation on CD16 effector functions[29,32] and recapitulate similar findings in the context of COVID-19[30,31]. However, we did not observe significant differences between critically and severely diseased patients.

COVID-19 disease severity correlates with an increase in CD16-reactive soluble IgG complexes.

Aside from afucosylation, it has been proposed that uncleared antigen-antibody immune complexes (ICs) might further exacerbate inflammation, explaining complications observed in COVID-19 such as cytokine storm, systemic vasculitis, microvascular thrombosis and organ

failure[33-35]. However, the presence of circulating, soluble ICs (sICs) in critically or severely diseased patients has not been conclusively shown yet. As extensive FcγR activation by sICs might contribute to the severe systemic inflammatory state occurring in some COVID-19 patients with prolonged disease, we surmised that sICs might be a putative explanation for the marked differences in IL-6, PCT and CRP levels between critically and severely diseased patients (Table 1). We thus set out to characterize our patient cohort regarding the presence of sICs in serum samples taken at various time points during disease and after hospitalization. To this end, we deployed a novel cell-based reporter assay developed to quantify CD16 (158V) activation by IgG-containing sICs[17]. As recently shown, the assay does not react to monomeric IgG or small dimeric complexes in solution, but specifically identifies multimeric sICs and has been successfully used to identify sICs in patients with systemic lupus erythematosus (SLE)[16]. Moreover, the assay is sensitive to sICs size with larger complexes leading to stronger receptor activation compared to small complexes. Analysis of serum samples, obtained 13-25 days after symptom onset, revealed the presence of highly CD16-reactive sICs in SARS-CoV-2 infected patients compared to healthy individuals (Figure 4A). Next, we compared sIC-mediated CD16 activation between COVID-19 patients of varying disease severity. While all COVID-19 patient groups tested positive for reactive sICs compared to healthy control (HD) sera, we found that critically diseased patients show a striking increase in reactive sICs compared to patients with severe or mild disease (Figure 4B). Only 6 out of 27 patients with critical disease (22%) showed no sIC-mediated CD16 activation. As we did not detect reactive sICs in the serum of 47 patients with acute respiratory distress syndrome (ARDS; mean age 57.5 years) in response to infections of different etiology including CMV reactivation, HIV, influenza or TBC infection, we conclude that the formation of reactive sICs is associated with severe SARS-CoV-2 disease (Figure 4-figure supplement 1). Longitudinal analysis of reactive sICs in the serum of critically or severely diseased patients revealed high CD16 activation levels in 4 critically diseased patients already 6 to 8 days after symptom onset (Figure 4C). Of note, 2 of 4 patients with an early increase of circulating reactive sIC eventually died. sIC-mediated CD16 activation persisted in 14 of 19 critically diseased patients at high levels until day 26 after symptom onset. sIC-mediated CD16 activation in severely diseased patients was slightly delayed compared to critically diseased patients and was first detected in 4 patients 9-11 days after symptom onset (Figure 4C). Only 4 of 14 patients with severe disease showed detectable sIC-mediated CD16 activation. To verify that sICs represent the CD16-reactive component in the serum of COVID-19 patients, we analyzed serum-mediated CD16 activation before and after

PEG8000-precipitation. This treatment was previously shown to selectively precipitate large IgG complexes from solution[36]. For this analysis, pools of 8 sera, showing either high (IC+) or no (IC-) CD16 activation, were compared. Sera from healthy donors (HD) served as a negative control. Compatible with the hypothesis of serum-derived sICs driving CD16 activation, no activation was observed following incubation with 3.5% PEG8000 (Figure 4-figure supplement 2 A). To ensure, that the treatment did not precipitate monomeric IgG, we tested the depleted sera for remaining S1- and N-specific IgG. As depicted S1- and N-specific IgG could still be detected at high levels in samples treated with 3.5% PEG8000 (Figure 4-figure supplement 2 B). When resolving sIC-mediated CD16 activation over the complete time of hospitalization for select patients from which samples at different time points were available, we observed that sIC reactivity follows a similar course as anti-S1 IgG titers in ELISA (Fig. 4-figure supplement 3). While this might imply that sIC formation involves SARS CoV-2 S1 antigen, we were not able to identify any SARS-COV-2-derived antigens in PEG8000-precipitated sICs using tandem mass spectrometry (data not shown). To further exclude the formation of multimeric sICs formed from circulating S1 antigen, we also specifically targeted S1 for precipitation from patient serum using biotinylated S1-specific monoclonal antibodies. However and in line with our previous approach, S1-specific precipitation using streptavidin-sepharose beads and subsequent mass spectrometry analysis for any SARS-CoV-2-specific antigens in sICs remained inconclusive (data not shown). Recently, the role of neutrophil mediated intravascular NETosis was found to play a critical role in thrombose formation and subsequent organ damage observed in severe clinical forms of COVID-19[37]. Since this process could mediate the formation of aggregated IgG as a form of sICs, we next tested whether Benzonase® nuclease treatment of patient serum would dissolve reactive sICs. To this end we tested sera from critically diseased patients or healthy individuals and compared CD16 reactivity before and after nuclease treatment (Figure 4-figure supplement 4). Nuclease activity in diluted human serum was controlled using plasmid DNA for reference. This revealed that nucleic acid was not involved in the formation of CD16-reactive sICs in critically diseased patients. Finally, we tested pooled patient sera for autoantibodies against a panel of prototypical autoantigens associated with autoimmune disease including anti-nuclear autoantibodies (ANA) by indirect immunofluorescence, dsDNA autoantibodies by ELISA and autoantibodies against the extractable nuclear antigens (nRNP/Sm, Sm, SS-A, Ro-52, SS-B, Scl-70, PM-Scl, Jo-1, CENP B, PCNA, nucleosomes, histones, ribosomal P-protein, AMA-M2, DFS70) by dot blot in case SARS-CoV-2 infection triggers autoantibody formation and possible sIC formation. However, no significant

autoantibody titers could be detected in any sera pool (data not shown). Although we were not able to identify their origin, our data clearly indicates the presence of circulating sICs in COVID-19 patients with an increase in CD16-reactive sICs corresponding with severity of disease. Accordingly, we conclude that circulating sICs are a hitherto unknown, yet contributing factor to COVID-19 disease severity and, regarding infectious diseases, our findings represent an observation unique to severely diseased COVID-19 patients.

Discussion

We collected and analyzed data from 41 COVID-19 patients hospitalized at the University Hospital Freiburg. Patients were categorized by severity of disease into severely (n=14) and critically diseased patients (n=27). Both groups were of comparable average age and had a similar male-to-female ratio. For comparison we also analyzed 28 mildly diseased and 30 healthy individuals. As key findings we identify the potential of *de novo* produced SARS-CoV-2 IgG and the presence of soluble immune complexes activating FcγRIII/CD16 as independent risk factors closely associated with severe courses of COVID-19.

CD16 activation by SARS-CoV-2 specific IgG is increased in critically diseased patients.

FcγR activation by anti-viral IgG represents a potent defense mechanism, directing the immune response to the site of viral replication[38-41]. However, persistent infection can lead to prolonged stimulation of FcγRs, driving an overshooting and potentially damaging inflammatory response[12,18]. A potential key component in prolonged inflammation following SARS-CoV-2 infection is FcγR mediated cytokine and chemokine release by several immune cells as their activation has been implied in severity of disease[29,31,42]. Along these lines, glycan profiles of anti-SARS-CoV2 IgG have been identified as major correlates of COVID-19 disease progression[29-31]. As these modifications particularly affect CD16 activation, we characterized our patient groups with regard to CD16 activation by S- and N-specific IgG and determined significantly increased CD16 activation by S, N and RBD specific IgG in sera from severely and critically diseased patients compared to mildly diseased patients. We further identified a higher level of afucosylation being indicative of COVID-19 severity, which is in line with previous studies[29-31], and now directly link this general observation to an increased CD16 activation. Taken together, we find that CD16 activation by SARS-CoV-2-specific IgG can be directly correlated to IgG glycan modifications and disease severity.

Circulating sICs contribute to COVID-19 disease severity

Based on the herein presented results identifying CD16 activation to be a major correlate of disease severity, we further explored this using an adapted FcγR activation assay optimized to measure soluble immune complexes (sICs)[17]. Indeed, we provide first evidence of such circulating sICs in the serum of COVID-19 patients and experimentally confirm previous hypotheses suggesting immune complexes as potential drivers of disease progression in COVID-19[33-35]. In fundamental contrast to opsonized antigens decorating virus-infected cells, sICs become distributed systemically. Thus constitutive activation of $CD16^+$ monocytes, granulocytes and NK cells could readily explain systemic responses which potentiate local inflammation in virus-infected tissues intensifying organ damage and dysfunction. Although the origin of the circulating immune complexes still remains elusive, we clearly show that the presence of IgG-containing sICs is restricted to SARS-CoV-2 infection and that complexed IgG is directly responsible and sufficient for the observed CD16 activation by patient serum. As we find sIC reactivity to roughly follow SARS-CoV2-S specific IgG responses, we speculated that circulating S or shed S1-antigens might still be involved in sIC formation, albeit in a form we were not able to detect. In support of this hypothesis, it has recently been published that circulating S-antigen can be detected in the plasma of individuals who received two doses of the mRNA-1273 (Moderna) vaccine[43]. S1 shedding was also reported to play a role in virion infectivity as the introduction of a D614G mutation significantly enhanced infectivity due to an increased S-protein density in the virion[44]. Finally, others have identified potential mechanisms leading to S-antigen shedding in viral infection and proposed a link between the presence of circulating S-antigen and disease severity[45]. Alternatively, IgG auto-antibodies of diverse specificity might cause the formation of the CD16 triggering sICs we herein identified. In fact, several studies have described that auto-antibodies can be frequently detected in critically ill COVID-19 patients[46-48]. In particular, very recent work shows that an acute SARS-CoV-2 infection triggers the *de novo* IgG production against multiple autoantigens. Interestingly, 60-80% of all hospitalized COVID-19 patients had anti-cytokine IgG (ACA)[49]. The authors show that ACA levels and specificity change over time during hospitalization, suggesting ACA induction in response to viral infection and inflammation. Further, it has been shown that pre-existing neutralizing anti-type I interferon antibodies, which can be found in about 10% of patients with severe COVID-19 pneumonia, are related to the highest risk of developing life-threatening COVID-19 disease[50]. Therefore, the *de novo* induction of anti-cytokine auto-antibodies in a large proportion of hospitalized COVID-19 patients as described by Chang et al[49], might indeed represent the origin of circulating sICs in

COVID-19. In such a scenario, immune responses are deviated first by depletion of important cytokines and second through the formation of pathological sICs which trigger immunological damage. We show that critically diseased patients show significantly higher levels of reactive sICs compared to less severely diseased patients. In addition, sIC responses can be found significantly earlier in critically diseased patients, which was associated with a fatal disease outcome. We also find that patients show a wide range of sIC reactivity. According to the Heidelberger-Kendall precipitation curve[51], sIC size is critically dependent on the antigen:antibody stoichiometry. As the used FcγR activation assay is sensitive to sIC size[17], it is highly likely that this also plays a role when measuring COVID-19 patient serum. As some patients show high anti-SARS-CoV-2-S IgG titers in the absence of sICs and vice versa we speculate that sIC size plays a role in CD16 reactivity. Therefore, we propose that in addition to the presence of sICs, the size of sICs plays a role in CD16 driven COVID-19 immunopathology.

Taken together, we conclude that CD16 activation in COVID-19 disease is governed by IgG glycan profiles and sIC formation (Figure 5) and plays a major role in disease progression and severity. Indeed, there is evidence in this direction from a clinical perspective provided by a recent study that finds the administration of intravenous immunoglobulin (IVIg) to alleviate COVID-19 disease[52]. Although no direct proof, this heavily implies that the saturation of FcγRs mitigates immunopathology. Therefore, our findings provide an explanation for the sustained immunopathology following SARS-CoV-2 infection as well as for the efficacy of IVIg treatment in severe to critical COVID-19 disease.

Material and Methods

Subjects and specimens

Between March 2020 and April 2020, 41 patients with SARS-CoV-2 infection confirmed by real-time PCR were hospitalized in the University Medical Center, Freiburg. Serum samples were collected during hospitalization for routine laboratory testing. Clinical data were obtained from electronic medical records. A total of 27 patients necessitating invasive mechanical ventilation were included in the critical group. Fourteen patients requiring O_2 supplementation were included in the severe group. Additionally, serum samples from 29 mild COVID-19 cases and 30 healthy donor (HD) plasma samples were used as controls in this study.

396

397 **Cell culture**

398 African green monkey kidney Vero E6 cells (ATCC CRL-1586) were cultured at 37°C in
399 Dulbecco's Modified Eagle Medium (DMEM) supplemented with 10% (vol/vol) fetal calf
400 serum (FCS, Biochrom), sodium pyruvate (1x, Gibco) and 100 U/ml penicillin-Streptomycin
401 (Gibco). BW5147 mouse thymoma cells (BW, obtained from ATCC: TIB-47) were stably
402 transduced with human FcγR as previously described[53]. Cells were maintained at $3x10^5$ to
403 $9x10^5$ cells/ml in Roswell Park Memorial Institute medium (RPMI GlutaMAX, Gibco)
404 supplemented with 10% (vol/vol) FCS, sodium pyruvate (1x, Gibco), 100 U/ml penicillin-
405 Streptomycin (Gibco) β-mercaptoethanol (0.1 mM, Gibco). Cells were cultured at 37°C, 5%
406 CO_2. All cell lines were routinely tested for mycoplasma.

407

408 **Monitoring of antibody response to SARS-CoV-2 by ELISA**

409 Serum IgG antibody titers targeting S1- and N-SARS-CoV-2 proteins were measured using
410 commercial enzyme-linked immunosorbent assay (ELISA). Anti-S1- SARS-CoV-2 IgG was
411 measured by the anti-SARS-CoV-2 ELISA (IgG) Euroimmune Kit (Euroimmune, Lübeck,
412 Germany) according to manufacturer's protocol. Results, expressed as arbitrary units (AU),
413 were evaluated semi-quantitatively by calculation of the ratio of the extinction of the control
414 or patient sample over the extinction of the calibrator. This ratio is interpreted as follows: <
415 0.8 negative; ≥ 0.8 to <1.0 borderline; ≥ 1.1 positive. Anti-N SARS-CoV-2 IgG was detected
416 using the recomWell SARS-CoV-2 IgG Kit (Mikrogen Diagnostik GmbH, Neuried,
417 Germany) according to manufacturer's protocol. The corresponding antibody activity
418 expressed in AU/ml is calculated using the formula (absorbance of sample / absorbance of
419 cut-off) × 20. Result are interpreted as follow: < 20 negative; ≥ 20 to < 24 borderline; > 24
420 positive. IgG against the SARS-CoV-2 Spike Glycoprotein Receptor Binding Domain (RBD)
421 were detected using SARS-CoV-2 IgG ELISA Reagent Set, kindly provided by InVivo
422 (InVivo Biotech Services GmbH, Hennigsdorf, Germany) according to manufacturer's
423 protocol.

424

425 **Fcγ receptor activation assay**

426 FcγRIIIA (CD16A, 158V) activation was measured by a cell-based assay as previously
427 described[28]. For detection of anti-S and anti-RBD-specific FcγR activation we utilized SARS-
428 CoV-2-S- and RBD-coated plates (kindly provided by InVivo Biotech Services GmbH,
429 Hennigsdorf, Germany). The recombinant (S)-protein was produced under serum-free

conditions in mammalian cells and contains amino acid residues 1 to 1213 of the SARS-CoV-2 Wuhan-Hu-1-isolate (GenBank annotation QHD43416.1). The furin cleavage site was mutated, two mutations for protein stabilization were included, and the C-terminal domain was replaced by a T4 trimerization sequence and a C-terminal hexa-His-Tag[54] The recombinant RBD-protein represented amino acids 319 to 541 of the (S)-protein mentioned before. Both recombinant proteins were purified using immobilized metal exchange chromatography (IMAC) and preparative SEC under standard conditions in a regulated environment. Microtiter plates were coated using 0.2 µg recombinant (S)-protein or RBD-protein per well. N-specific FcγR activation was determined using plates coated with SARS-CoV-2-N (Mikrogen Diagnostik GmbH, Neuried, Germany). Respective plates were subsequently incubated with serial dilutions of SARS-CoV-2 positive sera or control sera in RPMI supplemented with 10% (vol/vol) FCS for 30 min at 37°C. All wells were thoroughly washed before co-cultivation with BW5147 reporter cells for 16 h at 37°C, 5% CO_2. Cross-link activation of reporter cells was performed by direct coating of target antibody to ELISA plate (Nunc Maxisorp; 96 well, flat transparent), followed by a blocking step and incubation with 2×10^5 reporter cells per well. For all activation assays, mouse IL-2 secretion was quantified by anti-IL-2 ELISA, as described earlier. FcγRIIIA (CD16A) activation by sICs was measured by a recently developed cell-based assay[17]. Briefly, $2x10^5$ BW5147-CD16 reporter cells were incubated with SARS-CoV-2 sera in a total volume of 200 µl for 16 h at 37°C, 5% CO_2. Incubation was performed in a 96-well ELISA plate (Nunc Maxisorp) pre-treated with PBS containing10% FCS for 1 h at 4°C to avoid direct binding of serum IgG to the plate. Reporter cell mIL-2 secretion was quantified via ELISA as described previously[28].

Purification of SARS-CoV2-S and –N specific antibodies from serum

SARS-CoV-2-specific antibodies were purified using SARS-CoV-2 spike protein (S)-coated plates (kindly provided by InVivo BioTech Services) and - nucleocapsid (N) - coated plates recomWell SARS-CoV-2 IgG (Mikrogen Diagnostik GmbH, Neuried, Germany). Patient sera were diluted 1:5 in 100 µl (two wells per serum sample) and incubated for one hour at 37°C with the S- and N-precoated plates. After washing using PBS-T (0.05% Tween 20) 100 mM formic acid (30 µl/well) was added and incubated for 5 min on an orbital shaker at room temperature (RT) to elute bound IgG. Following pH neutralization using TRIS buffer (1 M), the eluates were either directly processed or stored at 4°C.

Quantitation of antigen-specific IgG amount

In order to determine the relative S1- and N-SARS-CoV-2 specific IgG antibody concentration of the generated eluates, S1- and N-ELISA were performed by the anti-SARS-CoV-2 ELISA (IgG) Euroimmune Kit (Euroimmune, Lübeck, Germany) and anti-N SARS-CoV-2 IgG ELISA (recomWell SARS-CoV-2 IgG Kit (Mikrogen Diagnostik GmbH, Neuried, Germany) as aformentioned.

Analysis of antigen-specific IgG-Fcγ fucosylation

Fucosylation levels of S- and N-specific IgG were measured using a lectin-based ELISA assay. Briefly, 96-well Maxisorb plates (Nunc®) were coated with 50µl/well anti-human IgG-Fab fragment (MyBiosource, MBS674607) at a concentration of 2 µg/ml, diluted in PBS for one hour at 37°C. After three washing steps with PBS-T (0.05% Tween20) unspecific binding sites were blocked adding 300 µl/well Carbo-free™ blocking solution (VectorLab, Inc., SP-5040, LOT: ZF0415) for one hour at room temperature. After three further washing steps, eluted antibodies were 2-fold serially diluted with PBS in a total volume of 30 µl/well and incubated for one hour at 37°C and 5% CO_2. After washing (3x) using PBS-T, 50 µl/well of 4 µg/ml biotinylated Aleuria Aurantia lectin (AAL, lectin, VectorLab, B-1395) diluted in lectin buffer (10 mM HEPES, 0.1 mM $CaCl_2$, 0.15 M NaCl, 0.1% Tween20) was added and incubated for 45 min at room temperature (RT). Following another three washing steps using PBS-T, Streptavidin-Peroxidase Polymer (Sigma, S 2438), at 1 µg/ml final concentration diluted in LowCross-HRP®-buffer (Candor, Order #.: 200 500) was added and incubated for one hour at RT. After washing five times with PBS-T, 50 µl/well of 1-Step™ Ultra TMB-ELISA Substrate Solution (ThermoFisher, 34028) was applied and the enzyme-substrate reaction was stopped after six minutes using 50 µl/well sulphuric acid (1 M H_2SO_4). Quantification of absorbance, OD_{450nm}, was performed using a Tecan M2000.

PEG Precipitation

Sera pools, consisting of eight different sera per pool, were diluted with varying amounts of PEG8000, in order to reach a final PEG8000 concentration of 1, 2, 3.5, 5 and 7.5% respectively. Mixtures were vortexed and incubated overnight at 4°C. For supernatant analysis, precipitates were sedimented via centrifugation at 13.000 rpm for 30 minutes at 4°C. For Mass Spectrometry analysis, PEG8000-precipitated sICs were shortly run into 10% polyacrylamide gels. After over-night fixation (40% ethanol, 10% acetic acid, 50% water) and washing (3x), complete lanes were excised.

Benzonase treatment of sera

Serum from six individual patients containing CD16-reactive soluble immune complexes, were treated with 250 units (U) of Benzonase Nuclease (Sigma-Aldrich Chemie Gmbh, Munich Germany) for 1 h at 4°C. After treatment, sera were titrated in complete BW5147 culture medium and tested for CD16 reactivity. Non-treated sera served as control. To verify Benzonase activity in the presence of human serum, 3 µg of pIRES-eGFP plasmid DNA (Addgene) were digested with 250 U of Benzonase. Successful nucleic acid digestion was visualized using a 1% agarose gel stained with Midori Green.

Immune precipitation

For mass spectrometry analysis of SARS-CoV2-S specific precipitates, individual sera containing CD16-reactive soluble immune complexes were subjected to immune precipitation (IP) using Pierce MS-compatible magnetic IP kit (ThermoFisher Scientific, Darmstadt, Germany) according to manufacturer's protocol. Briefly 250 µl serum was incubated overnight at 4°C with 5 µg of biotinylated anti-RBD-specific TRES-1-224.2.19 mouse monoclonal antibody or TRES-II-480 (isotype control) (kind gift of H.M. Jäck, Erlangen) before addition of streptavidin magnetic beads. Beads were subsequently collected via centrifugation and elution buffer was added to detach putative precipitated antigen. The elution was dried in a speed vacuum concentrator and shortly run into 10% polyacrylamide gels. After over-night fixation (40% ethanol, 10% acetic acid, 50% water) and washing (3x), complete lanes were excised. Antibody biotinylation was performed using a Pierce antibody biotinylation Kit for IP (ThermoFisher Scientific, Darmstadt, Germany) according to manufacturer's protocol.

Mass Spectrometry

Proteins were in-gel digested with sequencing grade modified trypsin (Promega GmbH, Walldorf, Germany) similar to the procedure described by Pandey et al.[55]. Vacuum-dried peptides were dissolved in 0.5% trifluoroacetic acid, loaded onto a trap column (C18 PepMap100, 5 µm particles, Thermo Fisher Scientific GmbH, Dreieich, Germany) with 0.05% trifluoroacetic acid (4 min, 10 µL/min) and separated on a C18 reversed phase column (SilicaTip™ emitter, 75 µm i.d., 8 µm tip, New Objective, Inc, Littleton, USA, manually packed 23 cm with ReproSil-Pur ODS-3, 3 µm particles, Dr. A. Maisch HPLC GmbH, Ammerbuch-Entringen, Germany; flow rate: 300 nL/min). For sample injection and multi-step gradient formation (eluent "A": 0.5% acetic acid in water; eluent "B": 0.5% acetic acid in

80% acetonitrile / 20% water; gradient length / acquisition time: 100 min or 175 min) an UltiMate 3000 RSLCnano system (Thermo Fisher Scientific GmbH, Dreieich, Germany) was used. Eluting peptides were electrosprayed at 2.3 kV via a Nanospray Flex ion source into a Q Exactive HF-X hybrid quadrupole-orbitrap mass spectrometer (both Thermo Fisher Scientific GmbH, Dreieich, Germany) and analyzed by data-dependent acquisition with HCD (higher energy collisional dissociation) fragmentation of doubly, triply and quadruply charged ions (loop count and dynamic exclusion dependent on the gradient length). Peak lists were generated with ProteoWizard msConvert (http://proteowizard.sourceforge.net/; version 3.0.11098), linear shift mass recalibrated (after a preliminary database search) using in-house developed software and searched against a database containing the SARS-CoV-2 UniProtKB reference proteome (proteome ID: UP000464024), all human UniProtKB/Swiss-Prot entries, and optionally (to reduce the number of incorrectly assigned matches) selected bacterial proteins (finally the Pseudomonas fluorescens (strain SBW25) reference proteome; proteome ID: UP000002332) with Mascot 2.6.2 (Matrix Science Ltd, London, UK; peptide mass tolerance: ± 5 ppm; fragment mass tolerance: ± 20 mmu; one missed trypsin cleavage and common variable modifications allowed).

Neutralization assay

Serum neutralization capacity was analyzed as previously described[56]. Briefly, VeroE6 cells were seeded in 12-well plates at a density of $2.8x10^5$ cells/well 24 h prior to infection. Serum samples were diluted at ratios of 1:16, 1:32 and 1:64 in 50 µL PBS total volume. Negative controls (PBS without serum) were included for each serum. Diluted sera and negative controls were subsequently mixed with 90 plaque forming units (PFU) of authentic SARS-CoV-2 (B.1) in 50 µl PBS (1600 PFU/mL) resulting in final sera dilution ratios of 1:32, 1:64, and 1:128. Following incubation at RT for 1 h, 400 µL PBS was added to each sample and the mixture was subsequently used to infect VeroE6 cells. After 1.5 h of incubation at RT, inoculum was removed and the cells were overlaid with 0.6% Oxoid-agar in DMEM, 20 mM HEPES (pH 7.4), 0.1% $NaHCO_3$, 1% BSA and 0.01% DEAE-Dextran. Cells were fixed 48h post-infection (4% formaldehyde for 30 minutes). Upon removal of the agar overlay, plaque neutralization was visualized using 1% crystal violet. PFU were counted manually. Plaques counted for serum-treated wells were compared to the average number of plaques in the untreated negative controls, which were set to 100%.

Statistical analyses

Statistical analyses were performed using linear statistical models. i.e. the two-group comparisons were made based on the t-statistic of the estimated effects. Differences over more than two groups were tested by Analysis of Variance (ANOVA) and multiple testing for subsequent two-group comparisons was then considered by performing Games-Howell post-hoc tests. For the time course data, patient differences were treated as random effects in a linear mixed effects model with time and clinical course (severe vs. critical) as fixed main and interaction effects. All analyses were performed at the $\log_2$ scale. Assumptions about variance heterogeneity and normal distribution were checked by visual inspection of diagnostic plots.

Ethics

The protocol of this study conforms to the ethical guidelines of the 1975 Declaration of Helsinki and was approved by the institutional ethical committee of the University of Freiburg (EK 153/20). Written informed consent was obtained from participants and the study was conducted according to federal guidelines, local ethics committee regulations (Albert-Ludwigs-Universität, Freiburg, Germany: No. F-2020-09-03-160428 and no. 322/20)

582 **Figure Legends**

583

584 **Figure 1**

585 **IgG responses against different SARS-CoV-2 proteins across severe and critical clinical**
586 **course of disease.**

587 IgG antibody levels were analyzed in longitudinal serum samples from hospitalized SARS-
588 CoV-2 infected individuals. 27 patients were categorized as critically diseased when in need
589 of invasive mechanical ventilation (red symbols) compared to 14 severely diseased patients
590 who did not require invasive ventilation (blue symbols). (A) IgG response against SARS-
591 CoV-2 S1 –protein and (B) SARS-CoV-2 N-protein as determined by commercial ELISA
592 assays. Dotted lines represent cut-off values for commercial S1- and N- specific ELISA
593 assays. Each dot represents the mean value obtained by the analysis of all samples which were
594 available at the indicated time points following symptom onset. Solid black lines indicate the
595 median. (C) Serum neutralization capacity against SARS-CoV-2 measured by a plaque
596 reduction assay. Sera were considered neutralizing upon 50% plaque reduction (dotted line) at
597 a 1:64 dilution. Solid black lines indicate the median. Significant differences were tested
598 using a linear mixed effects model (***, $p<0.001$; *, $p<0.05$).

599

600 **Figure 1-figure supplement 1**

601 **SARS-CoV-2 specific IgG levels in seronegative patients and according to disease**
602 **outcome.**

603 A) S1- and B) N-specific IgG levels in 30 healthy donors. Solid black lines indicate the
604 median. C) Cumulative S1-, D) N- and E) RBD-specific IgG levels measured 13-25 days after
605 symptom onset in deceased (black symbols) and not deceased COVID-19 patients (blue
606 symbols). Solid black lines indicate the median.

607

608 **Figure 1-figure supplement 2**

609 **Longitudinal changes in anti- SARS-CoV-2 IgG titers in severely and critically diseased**
610 **patients.**

611 Serial serum samples were collected from hospitalized COVID-19 patients and used for
612 SARS-CoV-2–specific IgG measurement. IgG responses against SARS-CoV-2 S1- and N-
613 protein in (A, C) critically (red symbols) and (B, D) severely (blue symbols) diseased patients.
614 Dotted lines represent cut-off values for commercial S1- and N- specific ELISA assays. Each
615 symbol represents the mean value of all samples which were available for each patient at the

indicated time range after symptom onset. There are no significant t-tests (i.e. $p>0.05$ for all comparisons).

Figure 2

CD16 activation by SARS-CoV-2 - specific IgG is enhanced in critically diseased patients.

FcγRIII activation by SARS-CoV-2-specific IgG on BW5147 reporter cells in serum samples obtained 13-25 days following symptom onset from 23 critically (red symbols) and 14 severely (blue symbols) diseased patients. Between 2 to 8 samples/patient were analyzed depending on the availability of sample material. Sera from 29 non-hospitalized patients with mild SARS-CoV-2 infection (grey symbols) and 30 healthy donors (open circles) served as reference. Each symbol represents the mean value of all available samples per patient. (A, B, C) ELISA levels for S1- N- and RBD-specific IgG. Dotted lines represent cut-off values for commercial S1-, N- and RBD - specific ELISA assays. Solid black lines indicate the mean. (D, E, F) FcγRIII activation by S-, N- and RBD-specific IgG expressed as log_2 fold change relative to negative control. Solid black lines indicate the mean. (G, H, I) FcγRIII activation, expressed as log_2 values relative to SARS-CoV-2-spcific IgG titers. Solid black lines indicate the mean. Significant differences over all three groups were tested by ANOVA and pairwise group comparison was made by Games-Howell post-hoc tests (***, $p<0.001$; **, $p<0.01$; *, $p<0.05$).

Figure 2-figure supplement 1

Cell-based reporter assay measuring CD16 activation in response to immobilized IgG and sICs. BW5147 reporter cells expressing chimeric human FcγRIII secrete IL-2 in response to FcγR activation by A) clustered viral specific IgG binding solid-phase antigen or B) soluble ICs. Solubility of sICs is achieved by pre-blocking an ELISA plate with PBS supplemented with 10% FCS as previously described[17].

Figure 2-figure supplement 2

Dose dependent CD16 activation by SARS-CoV-2 specific IgG.

CD16 activation by A) S- , B) N- and C) RBD-specific IgG in 9 representatively selected serum samples and one SARS-CoV-2 negative serum (dark blue bars). Sera were serially diluted at 1:20, 1:100, 1:500 and 1:2500. FcγRIII activation initiates IL-2 secretion by reporter cells, which is subsequently measured via ELISA (OD 450 nm). Based on this

empirical pretesting all sera were thereafter tested at 1:100 and 1:500 dilutions to reach an optimal dynamic range of response. The OD values obtained by the 1:500 dilutions were used for subsequent data analysis.

Figure 2-figure supplement 3

Reproducibility of CD16 activation measurements by SARS-CoV-2 specific IgG. Selected sera which were available in sufficient amount from patients with critical (red symbols) or severe (blue symbols) SARS-CoV-2 infection were tested in two independent experiments to show reproducibility and consistency of results. CD16 activation by S-, N- and RBD specific IgG is shown. Statistical tests using a Kolmogorov-Smirnov test indicate no significant differences.

Figure 2-figure supplement 4

Correlation of CD16 activation by virus specific IgG and ELISA levels.
Pearson's correlation coefficient was used to assess the relationship between virus–specific IgG levels and their capability to trigger CD16 activation on BW5147 reporter cells in 22 paired samples from patients with critical disease (red symbols), 14 paired samples from patients with severe disease (blue symbols) and 28 samples from patients with mild disease (grey symbols). Each dot represents the mean value obtained by the analysis of all samples available at the indicated time points. (A-C) anti-S IgG, (D-F) anti-N IgG and anti-RBD-IgG (E-I).

Figure 3

Anti SARS-CoV-2 IgG Fc core fucosylation in critical and severe COVID-19 cases.
IgG-Fc core fucosylation levels of SARS-CoV-2 –specific IgG in critically (red bars) and severely (blue bars) diseased COVID-19 patients. Analysis was carried out on a pool of 5 different sera. Measured OD values for fucosylation of the generated eluates were normalized to their respective IgG titers determined by antigen-specific S1 and N ELISA. A) S-IgG-Fc-fucosylation and B) N-IgG-Fc-fucosylation in critically and severely diseased patients characterized by either high (red) or low (patterned) CD16-activation levels in the FcγR activation reporter assay. The mean and standard deviation (SD) of at least three independent experiments is depicted. Statistical tests using a two-factorial linear model indicate three significant differences between the low and high categories (***, $p<0.001$; **, $p<0.01$; *, $p<0.05$; ns = not significant).

Figure 4

Severe COVID-19 disease coincides with high CD16 activation by sICs.

Serial serum samples obtained 13-25 days after onset of symptoms were analyzed in a cell-based reporter assay which is sensitive to sIC amount and size[16]. FcγR activation is shown as log_2 fold change relative to negative control. Each symbol represents the mean value obtained by the analysis of all samples available in the indicated time range for each individual patient. A) Analysis of CD16 activation by sICs in SARS-CoV-2-infected patients compared to healthy blood donors B) Levels of IC-mediated CD16 activation across severe, critical and mild clinical courses of COVID-19 disease, in healthy donors (HD) and in non-COVID-19-patients who developed acute respiratory distress syndrome (ARDS). Solid black lines indicate the mean. Two-group comparisons with the linear model indicate significant differences between critical cases and all other groups, as well as between severe cases and all other groups (***, $p<0.001$; **, $p<0.01$). No significant differences ($p>0.05$) have been found for the comparisons mild vs. healthy and for HD vs. ARDS. C) Kinetics of IC-mediated CD16 activation in critically and severely diseased patients. Solid black lines indicate the median. The mixed effects model indicates two time points with significant differences (**, $p<0.01$; *, $p<0.05$).

Figure 4-figure supplement 1

CD16 activation by sICs in non-COVID-19 patients with ARDS.

Serum samples from 47 patients with ARDS in response to infections of different etiology were analyzed in a cell-based reporter assay which is sensitive to sIC amount and size[16]. FcγR activation is shown as log_2 fold change relative to negative control. Each symbol represents one sample from one patient. CMV: Cytomegalovirus reactivation under immunosuppression; HIV: HIV infection; TBC: Mycobacterium tuberculosis infection; Influenza: influenza virus infection; TX: solid organ transplantation. Solid black lines indicate the median.

Figure 4-figure supplement 2

PEG precipitation eliminates sIC-mediated CD16 activation.

Pools of 8 sera were incubated with equal volumes of PEG8000 to reach the indicated final PEG concentrations. A) CD16 activation after PEG-precipitation in the pool supernatant, showing either high (sICs+) or no (sICs-) CD16 activation. Sera from healthy donors (HD) were included as a negative control. Activation levels are expressed as IL-2 levels (OD 450 nm) released by reporter cells. The mean and SD of two independent experiments is depicted.

718 B) Anti SARS-CoV-2 IgG levels against S1 (left panel) or N (right panel) IgG following PEG
719 precipitation. The mean and SD of two independent experiments (sIC+/sIC-) is depicted.
720
721 **Figure 4-figure supplement 3**
722 **Individual CD16 activation by sICs and anti-S1 ELISA IgG kinetics post symptoms**
723 **onset.**
724 Individual sera for either critically or severely diseased patients were analyzed in order to
725 detect anti S1-IgG antibodies (top panel) via Euroimmune ELISA [AU] and CD16 activation
726 by soluble immune complexes (lower panel, relative CD16 activation depicted as fold
727 increase to the negative control) over time (1-40 days post symptom onset). White panel: not
728 tested.
729
730 **Figure 4-figure supplement 4**
731 **Benzonase treatment of sIC-reactive sera does not abolish CD16 activation.**
732 Left panel: sIC-mediated CD16 reactivity expressed as $\log_2$ fold increase to the negative
733 control, in serum of six individual patients before and after treatment with 250 Units of
734 Benzonase Nuclease. Right panel: As positive control, 3 µg plasmid DNA was digested. M:
735 1kb DNA ladder, Lane 1: benzonase digestion in the presence of human serum, lane 2:
736 plasmid DNA w/o benzonase in the presence of human serum, lane 3: benzonase digestion in
737 medium only and lane 4: plasmid DNA w/o benzonase in medium only.
738
739
740 **Figure 5**
741 **Summary of antibody features from SARS-CoV-2-infected patients with critical and**
742 **severe disease.**
743 Relative multivariate antibody features illustrated as radar chart in critically (red) or severely
744 (blue) diseased COVID-19 patients normalized to the corresponding features of patients with
745 mild infection (grey). Each spoke represents one of the following variables: ELISA (S1-IgG,
746 N-IgG,) and CD16 activation (S-IgG, N-IgG, sICs). Arithmetic mean values of $\log_2$ values
747 were calculated for each group (days 13-25 post symptom onset) respectively. The fold
748 change compared to mildly diseased patients is shown.
749
750
751

752 **Table 1**

753 **Clinical characteristics of the hospitalized SARS-CoV-2 patients.**

754 Patients were categorized as either severely (hospitalized, requiring O_2 supplementation,
755 n=14) or critically diseased (hospitalized and in need of invasive mechanical ventilation,
756 n=27). Diagnostic markers are depicted as mean and SD (in brackets) of all analyzed
757 laboratory parameters obtained 13-25 days post symptom onset. Percentage [%] is indicated.

References

1 Zhu, N. *et al.* A Novel Coronavirus from Patients with Pneumonia in China, 2019. *N Engl J Med* **382**, 727-733, doi:10.1056/NEJMoa2001017 (2020).

2 Dong, E., Du, H. & Gardner, L. An interactive web-based dashboard to track COVID-19 in real time. *Lancet Infect Dis* **20**, 533-534, doi:10.1016/S1473-3099(20)30120-1 (2020).

3 Chen, G. *et al.* Clinical and immunological features of severe and moderate coronavirus disease 2019. *J Clin Invest* **130**, 2620-2629, doi:10.1172/JCI137244 (2020).

4 Felsenstein, S., Herbert, J. A., McNamara, P. S. & Hedrich, C. M. COVID-19: Immunology and treatment options. *Clin Immunol* **215**, 108448, doi:10.1016/j.clim.2020.108448 (2020).

5 Magleby, R. *et al.* Impact of SARS-CoV-2 Viral Load on Risk of Intubation and Mortality Among Hospitalized Patients with Coronavirus Disease 2019. *Clin Infect Dis*, doi:10.1093/cid/ciaa851 (2020).

6 Ruan, Q., Yang, K., Wang, W., Jiang, L. & Song, J. Correction to: Clinical predictors of mortality due to COVID-19 based on an analysis of data of 150 patients from Wuhan, China. *Intensive Care Med* **46**, 1294-1297, doi:10.1007/s00134-020-06028-z (2020).

7 Zhou, F. *et al.* Clinical course and risk factors for mortality of adult inpatients with COVID-19 in Wuhan, China: a retrospective cohort study. *Lancet* **395**, 1054-1062, doi:10.1016/S0140-6736(20)30566-3 (2020).

8 Yang, X. *et al.* Clinical course and outcomes of critically ill patients with SARS-CoV-2 pneumonia in Wuhan, China: a single-centered, retrospective, observational study. *Lancet Respir Med* **8**, 475-481, doi:10.1016/S2213-2600(20)30079-5 (2020).

9 Zhou, Y. *et al.* Pathogenic T-cells and inflammatory monocytes incite inflammatory storms in severe COVID-19 patients. *National Science Review* **7**, 998-1002, doi:10.1093/nsr/nwaa041 (2020).

10 Long, Q. X. *et al.* Antibody responses to SARS-CoV-2 in patients with COVID-19. *Nat Med* **26**, 845-848, doi:10.1038/s41591-020-0897-1 (2020).

11 Zhang, J. M. & An, J. Cytokines, inflammation, and pain. *Int Anesthesiol Clin* **45**, 27-37, doi:10.1097/AIA.0b013e318034194e (2007).

12 Vogelpoel, L. T., Baeten, D. L., de Jong, E. C. & den Dunnen, J. Control of cytokine production by human fc gamma receptors: implications for pathogen defense and autoimmunity. *Front Immunol* **6**, 79, doi:10.3389/fimmu.2015.00079 (2015).

13 Bruhns, P. & Jonsson, F. Mouse and human FcR effector functions. *Immunol Rev* **268**, 25-51, doi:10.1111/imr.12350 (2015).

14 Zubler, R. H. *et al.* Circulating and intra-articular immune complexes in patients with rheumatoid arthritis. Correlation of 125I-Clq binding activity with clinical and biological features of the disease. *J Clin Invest* **57**, 1308-1319, doi:10.1172/JCI108399 (1976).

15 Levinsky, R. J. Role of circulating soluble immune complexes in disease. *Arch Dis Child* **53**, 96-99, doi:10.1136/adc.53.2.96 (1978).

16 Levinsky, R. J., Cameron, J. S. & Soothill, J. F. Serum immune complexes and disease activity in lupus nephritis. *Lancet* **1**, 564-567, doi:10.1016/s0140-6736(77)91998-5 (1977).

17 Chen, H. *et al.* FcγR responses to soluble immune complexes are governed by solubility and size. *bioRxiv*, 2020.2011.2011.378232, doi:10.1101/2020.11.11.378232 (2021).

18 Wang, T. T. & Ravetch, J. V. Immune complexes: not just an innocent bystander in chronic viral infection. *Immunity* **42**, 213-215, doi:10.1016/j.immuni.2015.01.022 (2015).

19 Carreno, L. J., Pacheco, R., Gutierrez, M. A., Jacobelli, S. & Kalergis, A. M. Disease activity in systemic lupus erythematosus is associated with an altered expression of low-affinity Fc gamma receptors and costimulatory molecules on dendritic cells. *Immunology* **128**, 334-341, doi:10.1111/j.1365-2567.2009.03138.x (2009).

20 Faik, I. *et al.* Pyruvate Kinase and Fcgamma Receptor Gene Copy Numbers Associated With Malaria Phenotypes. *J Infect Dis* **216**, 276-282, doi:10.1093/infdis/jix284 (2017).

21 Xu, Z. *et al.* Pathological findings of COVID-19 associated with acute respiratory distress syndrome. *Lancet Respir Med* **8**, 420-422, doi:10.1016/S2213-2600(20)30076-X (2020).

22 Channappanavar, R. & Perlman, S. Pathogenic human coronavirus infections: causes and consequences of cytokine storm and immunopathology. *Seminars in Immunopathology* **39**, 529-539, doi:10.1007/s00281-017-0629-x (2017).

23 Smits, S. L. *et al.* Exacerbated innate host response to SARS-CoV in aged non-human primates. *PLoS Pathog* **6**, e1000756, doi:10.1371/journal.ppat.1000756 (2010).

24 Rockx, B. *et al.* Early upregulation of acute respiratory distress syndrome-associated cytokines promotes lethal disease in an aged-mouse model of severe acute respiratory syndrome coronavirus infection. *J Virol* **83**, 7062-7074, doi:10.1128/JVI.00127-09 (2009).

25 Hoepel, W. *et al.* High titers and low fucosylation of early human anti-SARS-CoV-2 IgG promote inflammation by alveolar macrophages. *Sci Transl Med* **13**, doi:10.1126/scitranslmed.abf8654 (2021).

26 Zohar, T. & Alter, G. Dissecting antibody-mediated protection against SARS-CoV-2. *Nat Rev Immunol* **20**, 392-394, doi:10.1038/s41577-020-0359-5 (2020).

27 Lu, L. L., Suscovich, T. J., Fortune, S. M. & Alter, G. Beyond binding: antibody effector functions in infectious diseases. *Nat Rev Immunol* **18**, 46-61, doi:10.1038/nri.2017.106 (2018).

28 Corrales-Aguilar, E. *et al.* A novel assay for detecting virus-specific antibodies triggering activation of Fe gamma receptors. *J Immunol Methods* **387**, 21-35, doi:10.1016/j.jim.2012.09.006 (2013).

29 Chakraborty, S. *et al.* Proinflammatory IgG Fc structures in patients with severe COVID-19. *Nat Immunol* **22**, 67-73, doi:10.1038/s41590-020-00828-7 (2021).

30 High titers and low fucosylation of early human anti-SARS-CoV-2 IgG promote inflammation by alveolar macrophages. *Sci Transl Med*, doi:10.1126/scitranslmed.abf8654 (2021).

31 Larsen, M. D. *et al.* Afucosylated IgG characterizes enveloped viral responses and correlates with COVID-19 severity. *Science* **371**, doi:10.1126/science.abc8378 (2021).

32 Li, T. *et al.* Modulating IgG effector function by Fc glycan engineering. *Proceedings of the National Academy of Sciences of the United States of America* **114**, 3485-3490, doi:10.1073/pnas.1702173114 (2017).

33 Roncati, L. *et al.* Type 3 hypersensitivity in COVID-19 vasculitis. *Clinical Immunology* **217**, doi:ARTN 108487
10.1016/j.clim.2020.108487 (2020).

34 Roe, K. High COVID-19 virus replication rates, the creation of antigen-antibody immune complexes and indirect haemagglutination resulting in thrombosis. *Transbound Emerg Dis* **67**, 1418-1421, doi:10.1111/tbed.13634 (2020).

35 Zhang, Y. *et al.* Coagulopathy and Antiphospholipid Antibodies in Patients with Covid-19. *N Engl J Med* **382**, e38, doi:10.1056/NEJMc2007575 (2020).

36 Creighton, W. D., Lambert, P. H. & Miescher, P. A. Detection of antibodies and soluble antigen-antibody complexes by precipitation with polyethylene glycol. *J Immunol* **111**, 1219-1227 (1973).

37 Veras, F. P. *et al.* SARS-CoV-2-triggered neutrophil extracellular traps mediate COVID-19 pathology. *J Exp Med* **217**, doi:10.1084/jem.20201129 (2020).

38 Horwitz, J. A. *et al.* Non-neutralizing Antibodies Alter the Course of HIV-1 Infection In Vivo. *Cell* **170**, 637-648 e610, doi:10.1016/j.cell.2017.06.048 (2017).

39 Forthal, D. N. & Moog, C. Fc receptor-mediated antiviral antibodies. *Curr Opin HIV AIDS* **4**, 388-393, doi:10.1097/COH.0b013e32832f0a89 (2009).

40 DiLillo, D. J., Tan, G. S., Palese, P. & Ravetch, J. V. Broadly neutralizing hemagglutinin stalk-specific antibodies require FcgammaR interactions for protection against influenza virus in vivo. *Nat Med* **20**, 143-151, doi:10.1038/nm.3443 (2014).

41 Hessell, A. J. *et al.* Fc receptor but not complement binding is important in antibody protection against HIV. *Nature* **449**, 101-104, doi:10.1038/nature06106 (2007).

42 Li, K. *et al.* Dynamic changes in anti-SARS-CoV-2 antibodies during SARS-CoV-2 infection and recovery from COVID-19. *Nature communications* **11**, 6044, doi:10.1038/s41467-020-19943-y (2020).

43 Ogata, A. F. *et al.* Circulating SARS-CoV-2 Vaccine Antigen Detected in the Plasma of mRNA-1273 Vaccine Recipients. *Clin Infect Dis*, doi:10.1093/cid/ciab465 (2021).

44 Zhang, L. *et al.* SARS-CoV-2 spike-protein D614G mutation increases virion spike density and infectivity. *Nature communications* **11**, 6013, doi:10.1038/s41467-020-19808-4 (2020).

45 Letarov, A. V., Babenko, V. V. & Kulikov, E. E. Free SARS-CoV-2 Spike Protein S1 Particles May Play a Role in the Pathogenesis of COVID-19 Infection. *Biochemistry (Mosc)* **86**, 257-261, doi:10.1134/S0006297921030032 (2021).

46 Woodruff, M. C. *et al.* Extrafollicular B cell responses correlate with neutralizing antibodies and morbidity in COVID-19. *Nat Immunol* **21**, 1506-1516, doi:10.1038/s41590-020-00814-z (2020).

47 Wang, E. Y. *et al.* Diverse functional autoantibodies in patients with COVID-19. *Nature*, doi:10.1038/s41586-021-03631-y (2021).

48 Zuo, Y. *et al.* Prothrombotic autoantibodies in serum from patients hospitalized with COVID-19. *Sci Transl Med* **12**, doi:10.1126/scitranslmed.abd3876 (2020).

49 Chang, S. E. *et al.* New-Onset IgG Autoantibodies in Hospitalized Patients with COVID-19. *medRxiv*, doi:10.1101/2021.01.27.21250559 (2021).

50 Bastard, P. *et al.* Autoantibodies against type I IFNs in patients with life-threatening COVID-19. *Science* **370**, doi:10.1126/science.abd4585 (2020).

51 Heidelberger, M. & Kendall, F. E. A Quantitative Study of the Precipitin Reaction between Type Iii Pneumococcus Polysaccharide and Purified Homologous Antibody. *J Exp Med* **50**, 809-823, doi:10.1084/jem.50.6.809 (1929).

52 Gharebaghi, N., Nejadrahim, R., Mousavi, S. J., Sadat-Ebrahimi, S. R. & Hajizadeh, R. The use of intravenous immunoglobulin gamma for the treatment of severe coronavirus disease 2019: a randomized placebo-controlled double-blind clinical trial. *BMC Infect Dis* **20**, 786, doi:10.1186/s12879-020-05507-4 (2020).

53 Kolb, P. *et al.* Identification and Functional Characterization of a Novel Fc Gamma-Binding Glycoprotein in Rhesus Cytomegalovirus. *J Virol* **93**, doi:10.1128/JVI.02077-18 (2019).

54 Amanat, F. *et al.* A serological assay to detect SARS-CoV-2 seroconversion in humans. *Nat Med* **26**, 1033-1036, doi:10.1038/s41591-020-0913-5 (2020).

55 Pandey, A., Andersen, J. S. & Mann, M. Use of mass spectrometry to study signaling pathways. *Sci STKE* **2000**, pl1, doi:10.1126/stke.2000.37.pl1 (2000).

56 Tönshoff, B. *et al.* Prevalence of SARS-CoV-2 Infection in Children and Their Parents in Southwest Germany. *JAMA Pediatrics* **175**, 586-593, doi:10.1001/jamapediatrics.2021.0001 (2021).

Acknowledgements

We thank Sophia Ruben and Torsten Schulz from InVivo Bio Tech Services for peparing SARS-CoV-2 (S)- and RBD- coated plates and preparing the SARS-CoV-2 IgG ELISA Reagent Set. We thank Hans-Martin Jäck for providing TRES-1-224.2.19 and TRES-II-480 monoclonal antibodies and Quinnlan David for critically reading the manuscript. We also thank Andreas Schlosser for validation of our Mass Spectrometry data. This work was supported by the Bundesministerium fuer Bildung und Forschung (BMBF) through the Deutsches Zentrum fuer Luft- und Raumfahrt, Germany, (DLR, grant number 01KI2077) and by the Federal State of Baden-Wuerttemberg, Germany, MWK-Sonderfoerdermaßnahme COVID-19/AZ.:33-7533.-6-21/7/2 to MS. This work was also supported by an intramural junior investigator fund of the Faculty of Medicine to PK (Hans A. Krebs - Funding for Medical Scientists, Faculty of Medicine, University of Freiburg) and "NaFoUniMedCovid19" (FKZ: 01KX2021 - COVIM to H.H., FKZ 100493916 B-FAST to H.H.) and DFG HE2526/9-1 to H.H.. A. Lother is a member of SFB1425, funded by the Deutsche Forschungsgemeinschaft (DFG, German Research Foundation #422681845). The funders had no role in the study design, data analysis, data interpretation, and in the writing of this report. All authors had full access to the data in the study and accept responsibility to submit for publication.

Author contribution:

Conceived and designed the experiments: J.A., A.M-P., S.G., P.K., A.L, V.F., M.S., H.H.

Performed the experiments: J.A., N.G., U.S., S.G., K. C., W.B.

Analyzed the data: J.A., S.G., P.K., V.F., K.C., A.M-P., W.B., C.K.

Contributed/reagent/sample material: A.B.G., D.H., T.W., N.G.M.

Writing and original draft preparation: J.A., S.G., P.K., V.F.

927

928 Review and editing: H.H., M.S., K.C.

929 Conceptualization: V.F., H.H.

930

931 **Competing interests:** The authors declare the following competing financial interest(s):
932 InVivo BioTech Services is a biotechnology company producing antibodies and proteins,
933 including SARS-CoV-2 antigens.

934 **Data and materials availability:** All data associated with this study are present in the paper
935 or Supplementary Materials.

936

Figures and Tables

Table 1

	All patients n: 41	%	critical n: 27	%	severe n: 14	%
Age [years]	Ø 68 (31-90)	-	Ø 63 (39-79)	-	Ø 76 (31-90)	-
Female	8	19.5	5	18.5	3	21.4
Male	33	80.5	22	81.5	11	78.6
Comorbidities						
Hypertension	21	51.2	12	44.4	9	64.3
Cardiovascular disease	14	34.1	5	18.5	9	64.3
Pulmonary disease	6	14.6	2	7.4	4	28.6
Chronic kidney disease	6	14.6	1	3.7	5	35.7
Diabetes	10	24.4	6	22.2	4	28.6
Malignancy	8	19.5	4	14.8	4	28.6
none	6	14.6	6	22.2	0	0
Diagnostic markers						
Interleukin-6 [pg/ml] Ø	1012.8	-	1452.1 (3774.6)	-	46.1 (26.8)	-
Procalcitonin [ng/ml] Ø	7	-	9.9 (21.9)	-	0.17 (0.11)	-
C- reactive protein [mg/l] Ø	128.1	-	162.2 (75.8)	-	65.3 (47.1)	-
Complications						
Bacterial superinfection	16	39	11	40.7	5	35.7
Treatment						
Hydroxychloroquine, Ritonavir+ Lopinavir (Kaletra®)	24	58.5	18	66.7	6	42.9
Fatal outcome						
Total	11	26.8	10	37	1	7.1

942 **Figure 1**

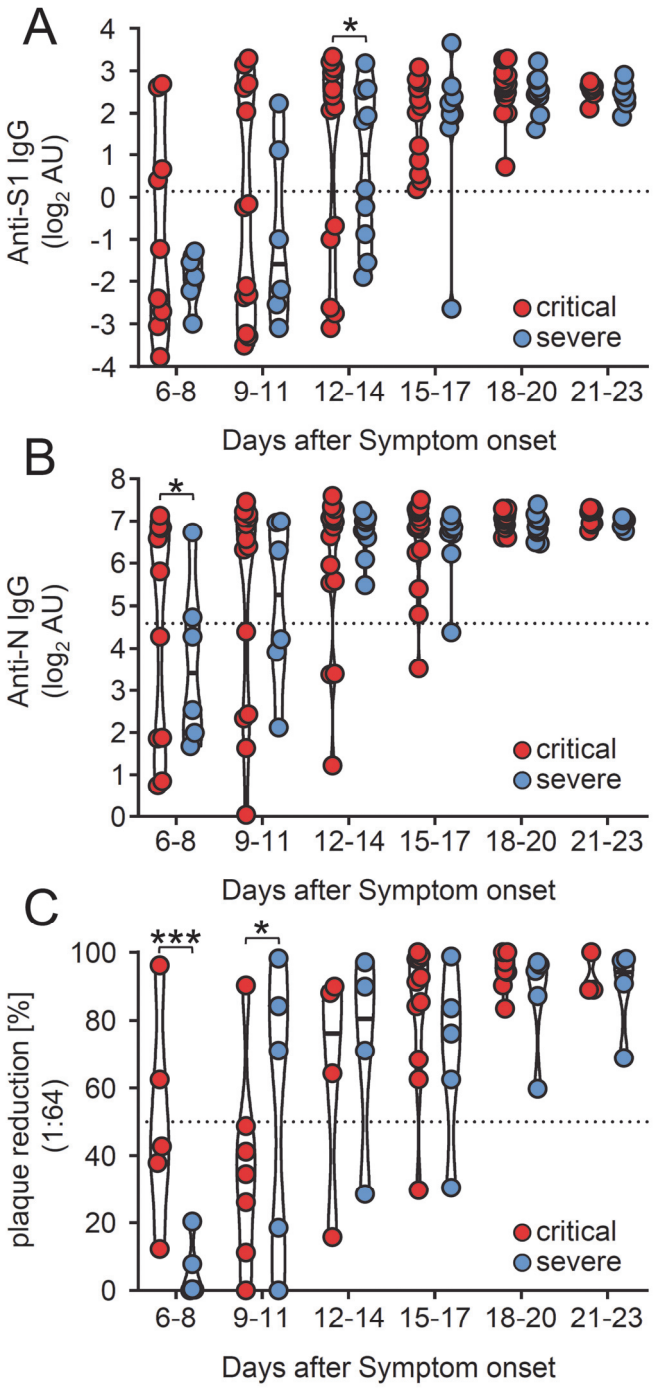

943

944

945

946 **Figure 1 – figure supplement 1**

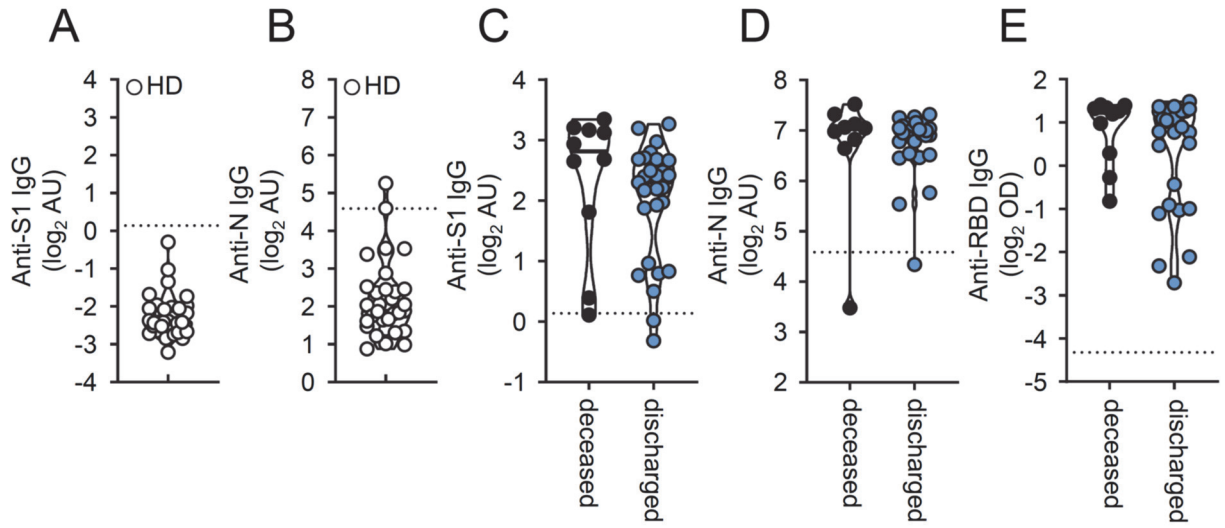

947

948

949 **Figure 1 – figure supplement 2**

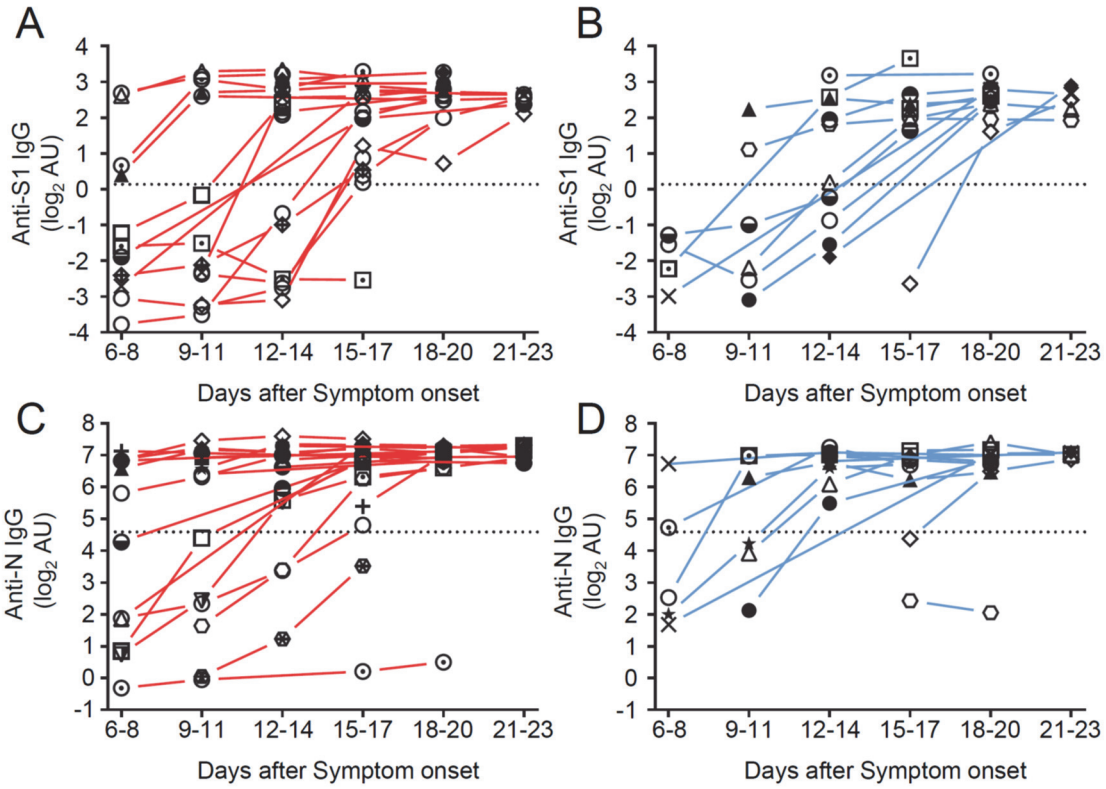

950

Figure 2

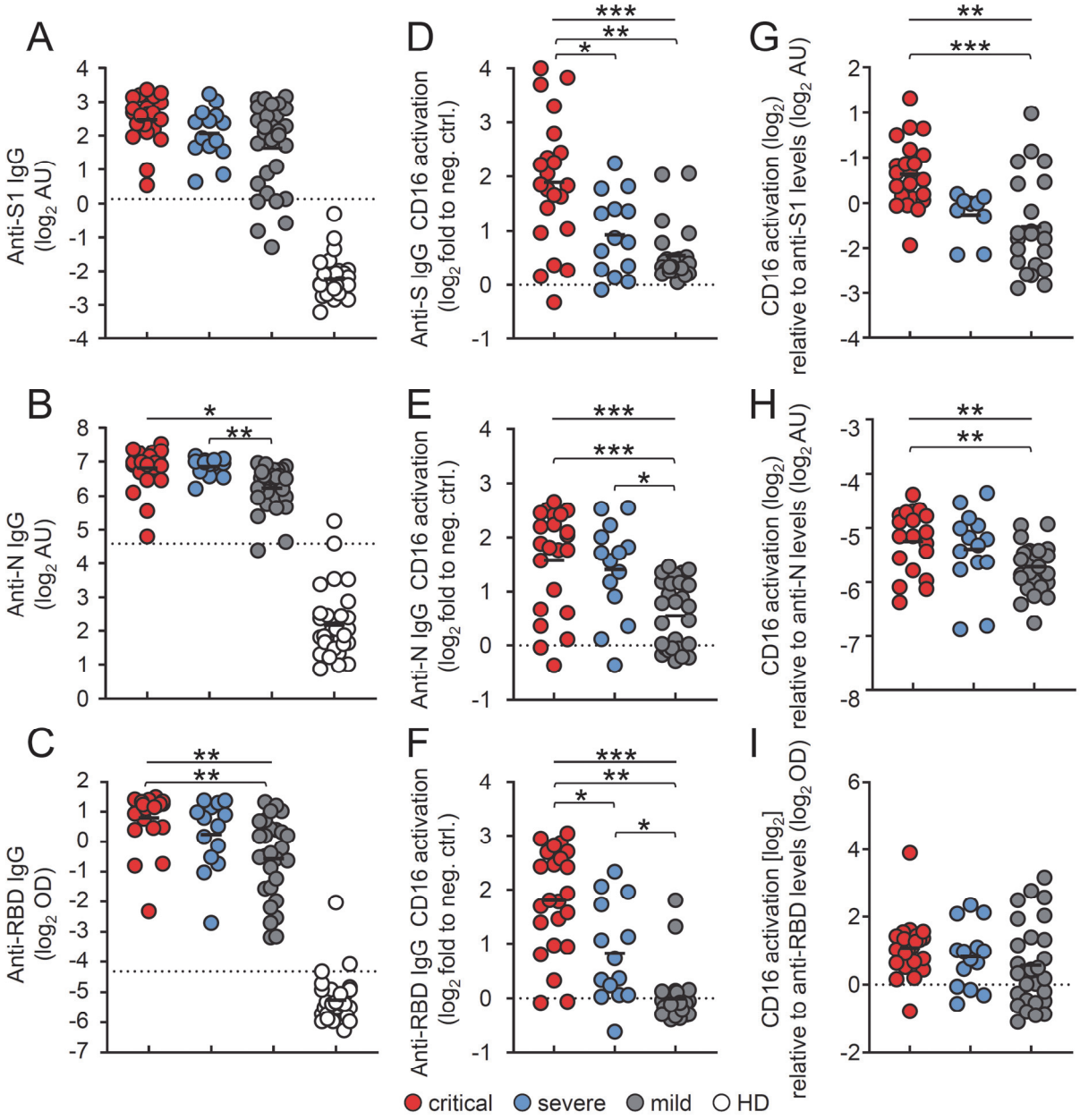

954 **Figure 2 –figure supplement 1**

955

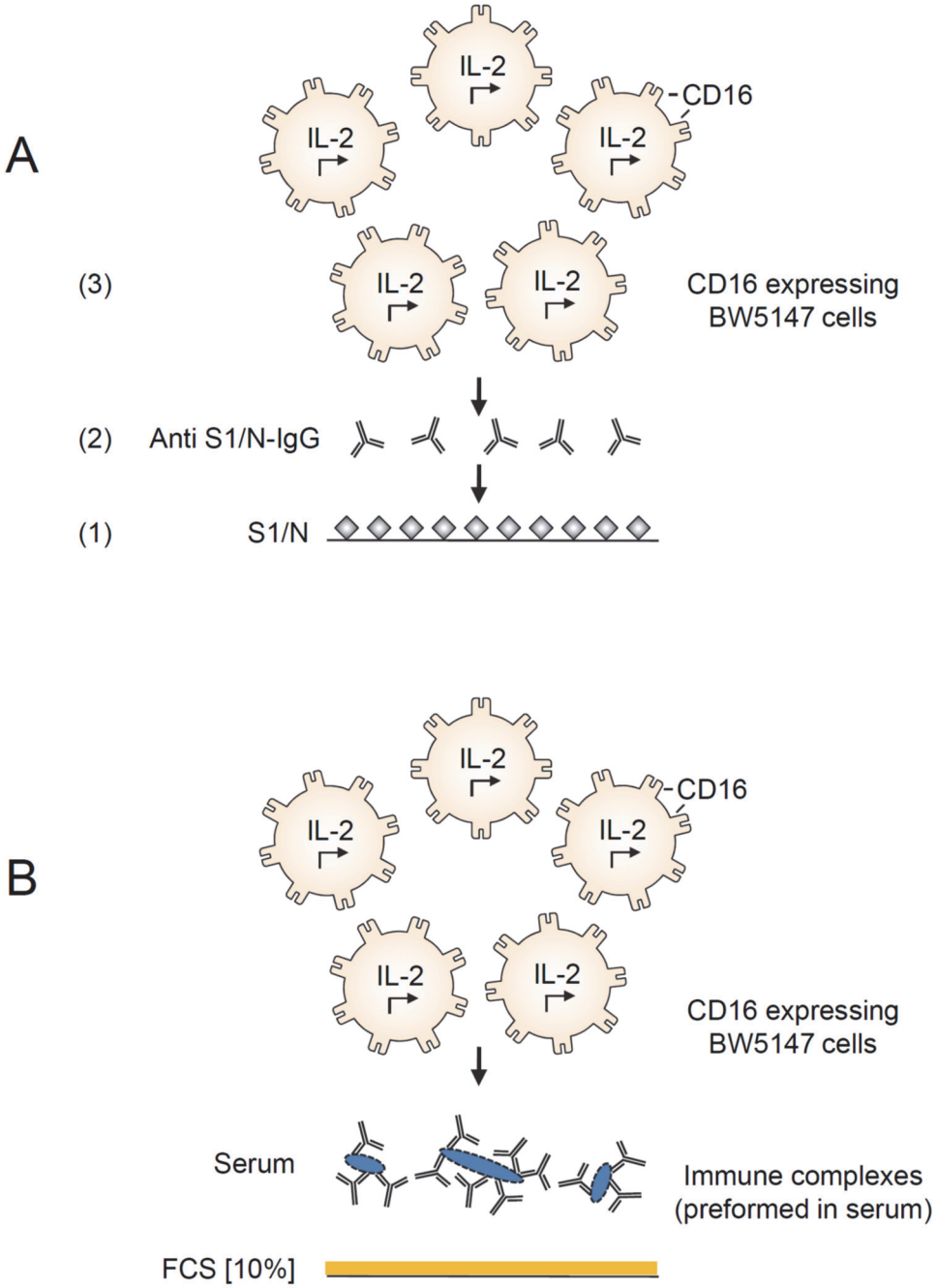

956

957

958 **Figure 2 –figure supplement 2**

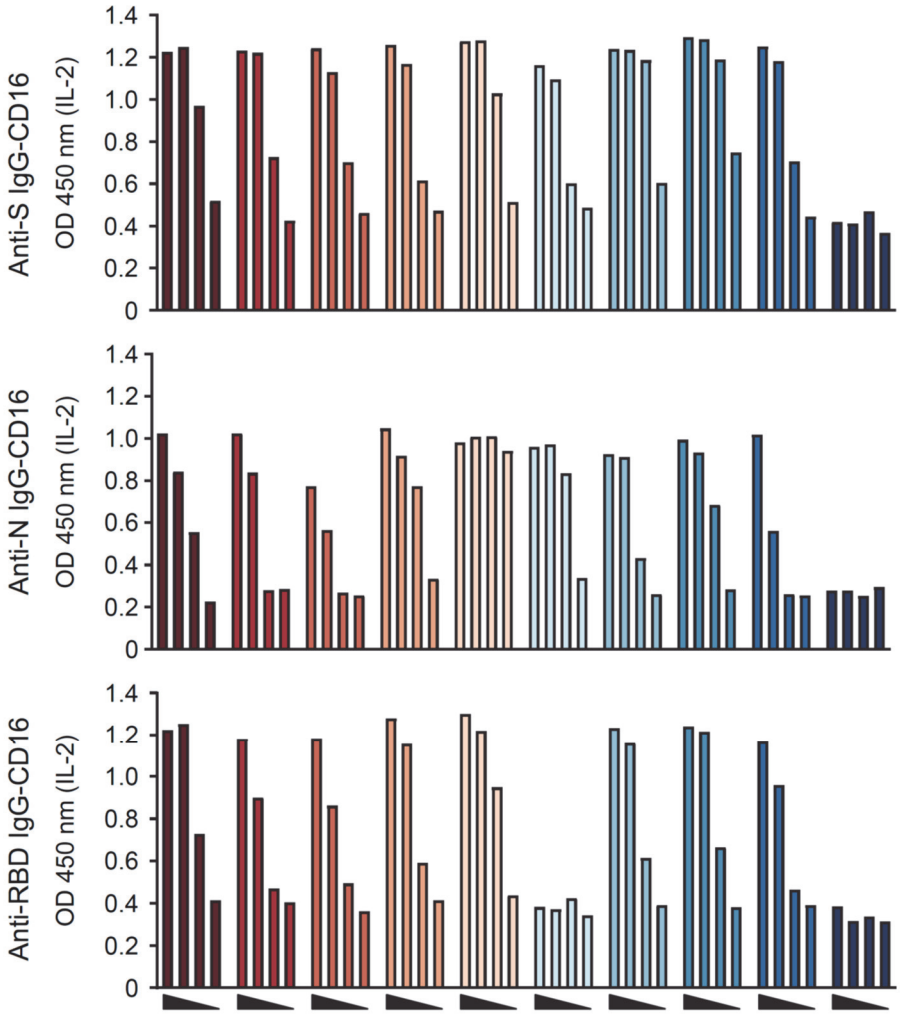

959

960

961 **Figure 2 –figure supplement 3**

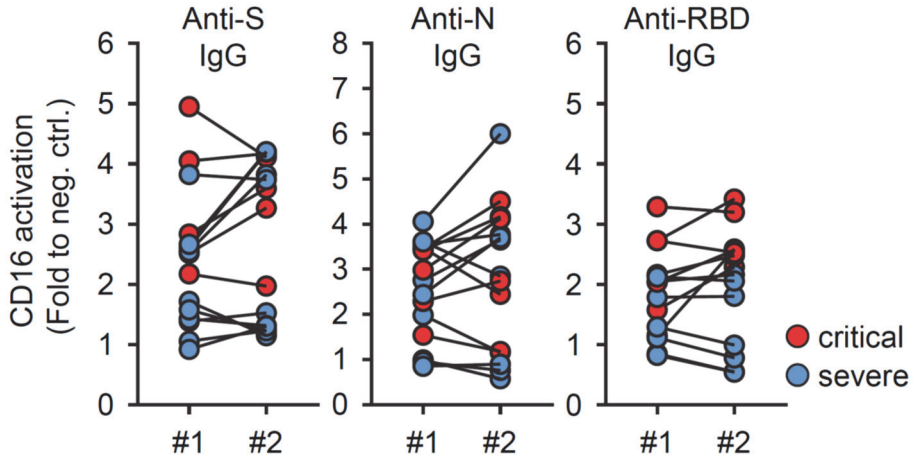

962

963

964 **Figure 2 –figure supplement 4**

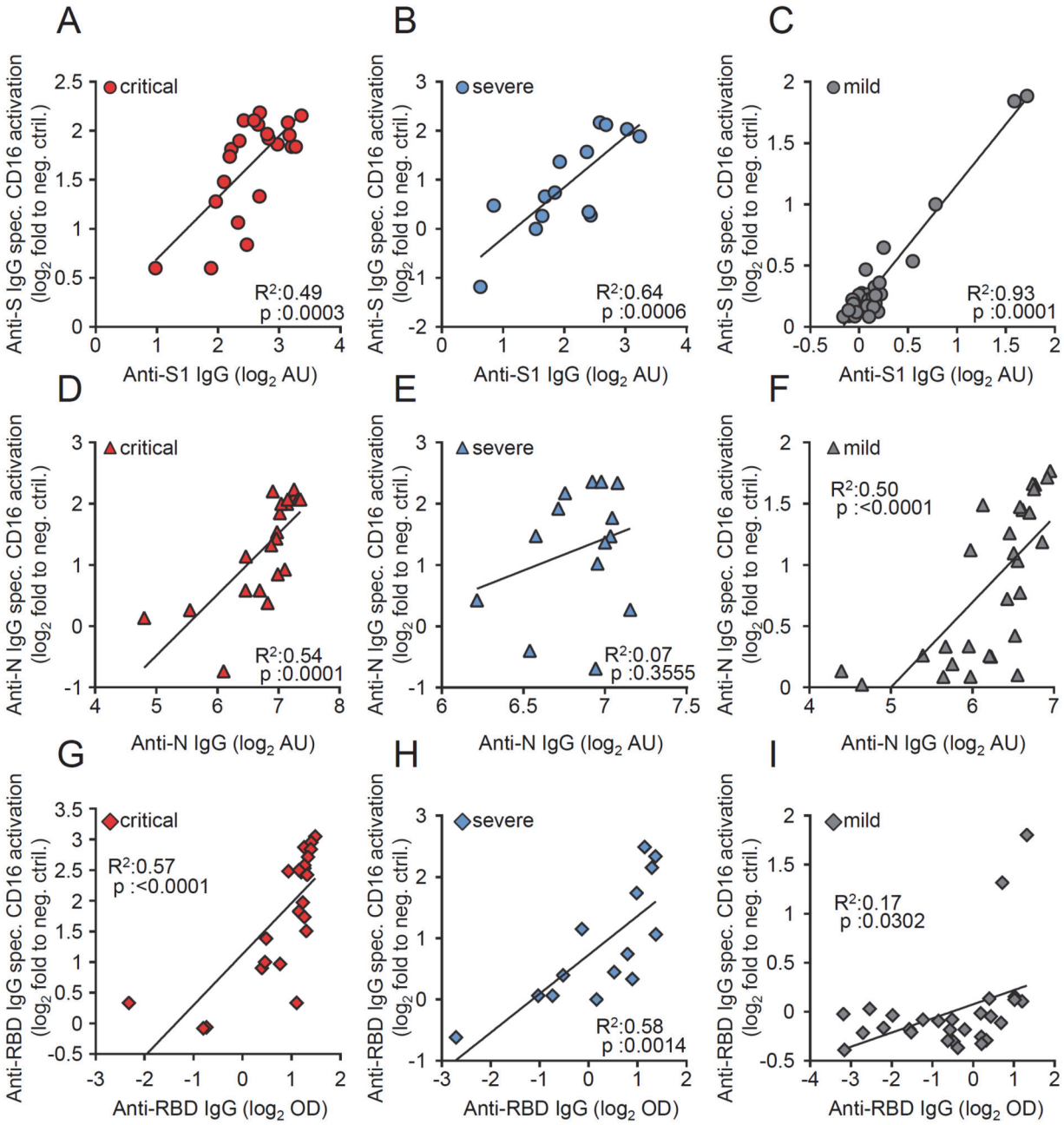

965

966

967 **Figure 3**

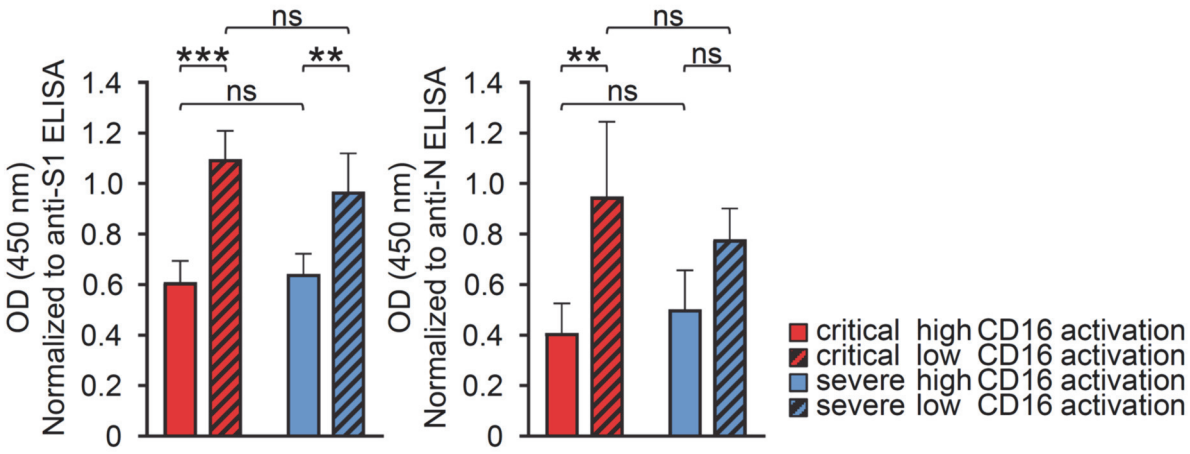

968

969

970 **Figure 4**

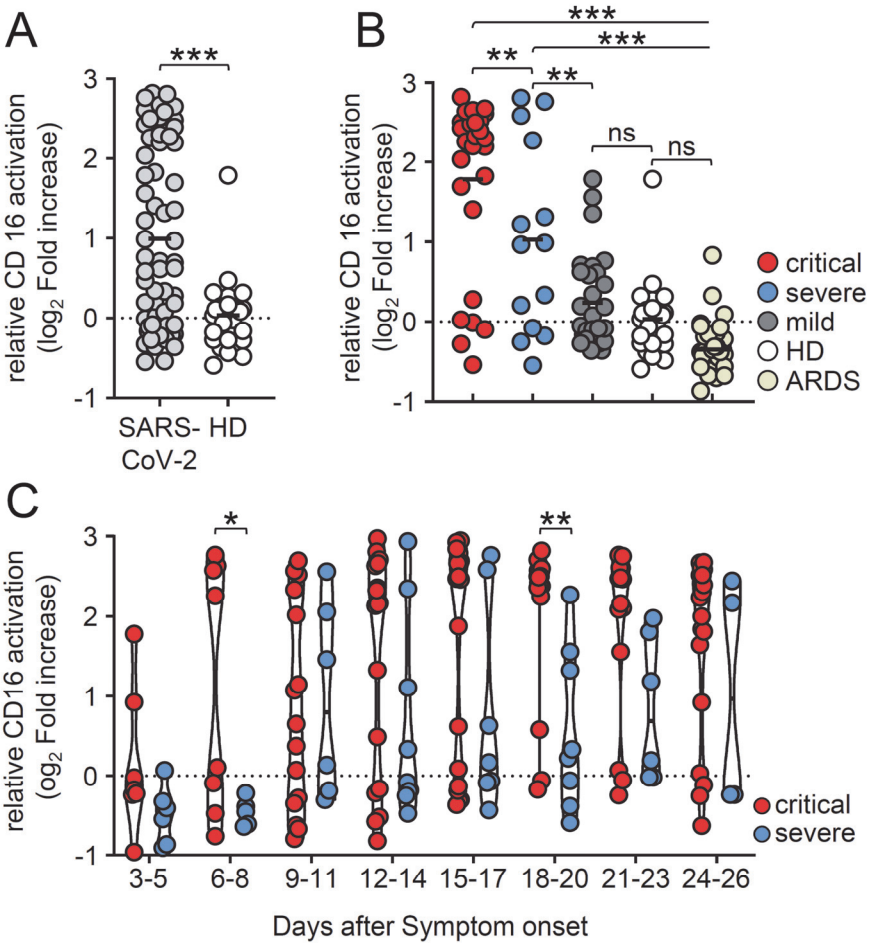

971

972

973 **Figure 4 – figure supplement 1**

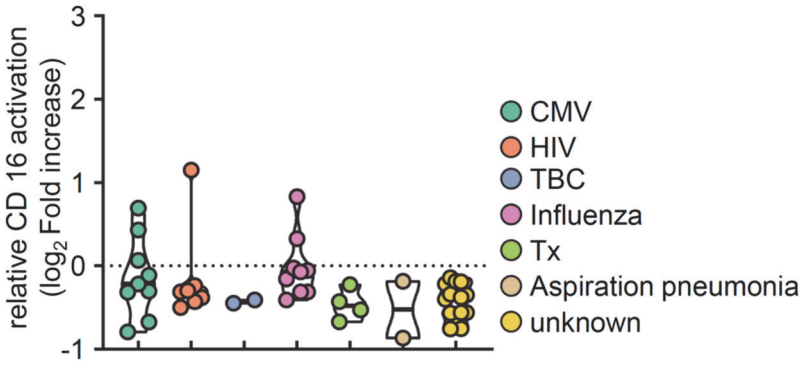

974

975

976 **Figure 4 – figure supplement 2**

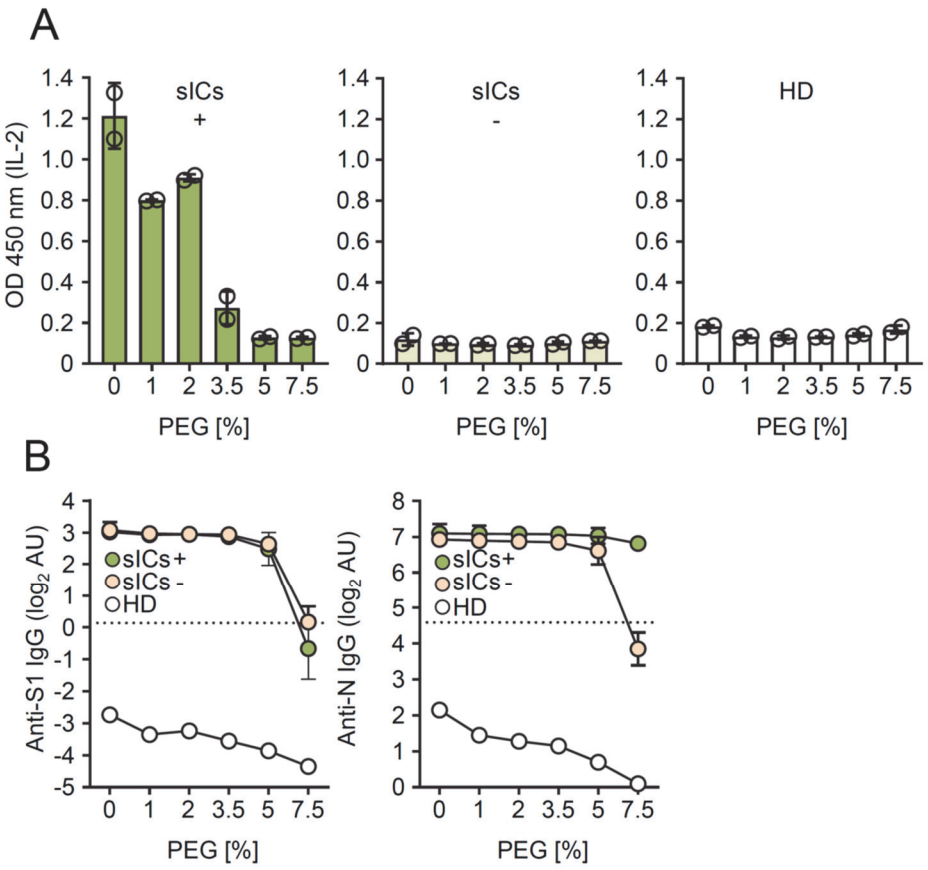

977

978 **Figure 4 – figure supplement 3**

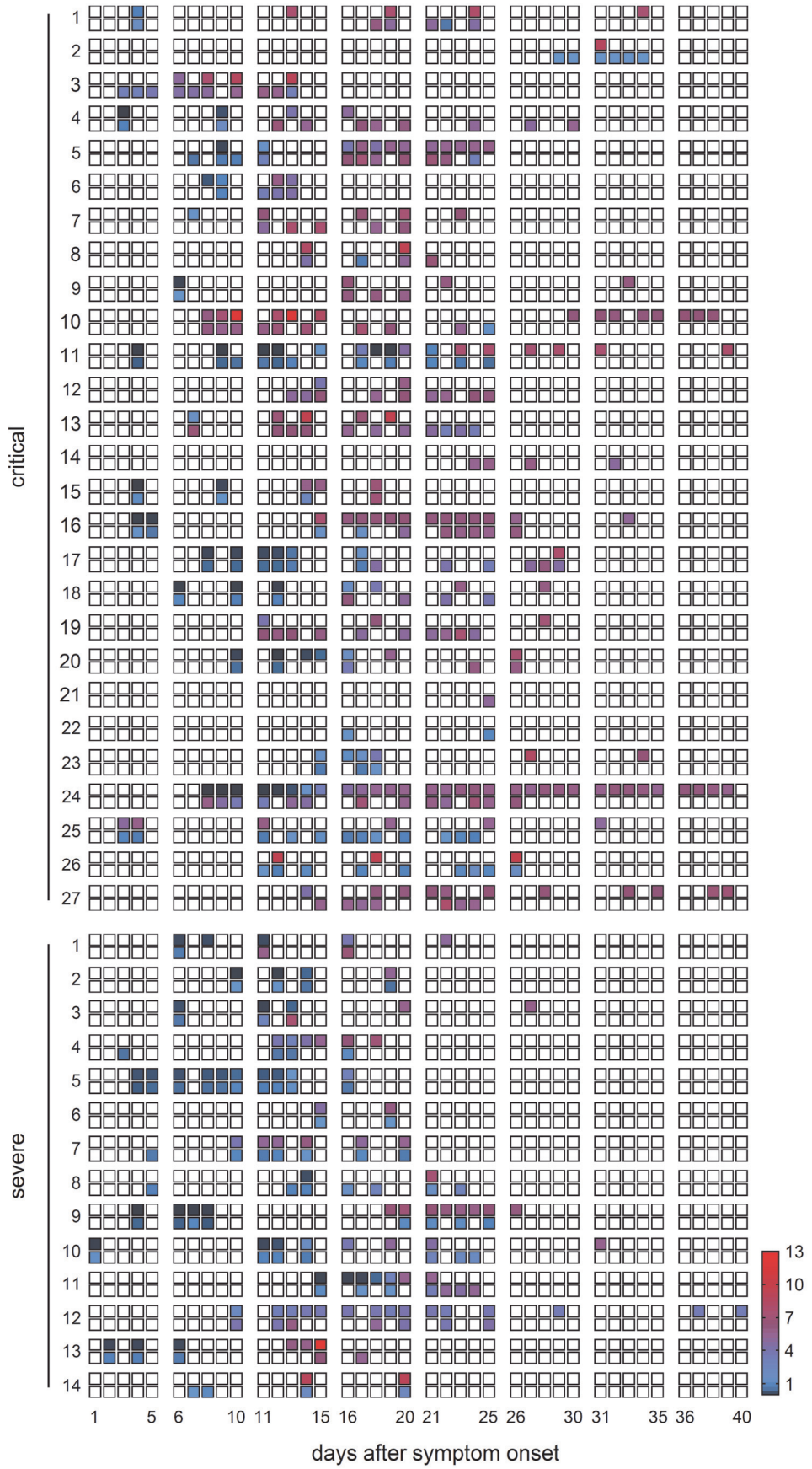

979

980 **Figure 4 – figure supplement 4**

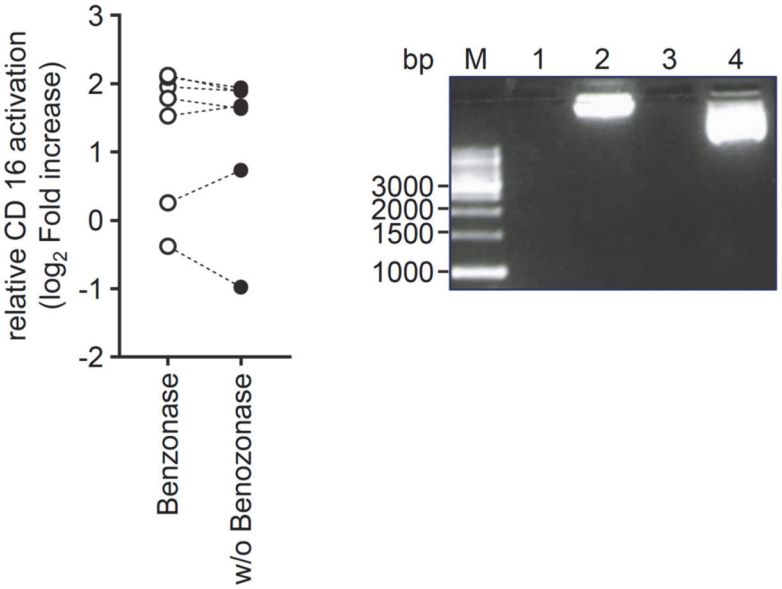

981

982 **Figure 5**

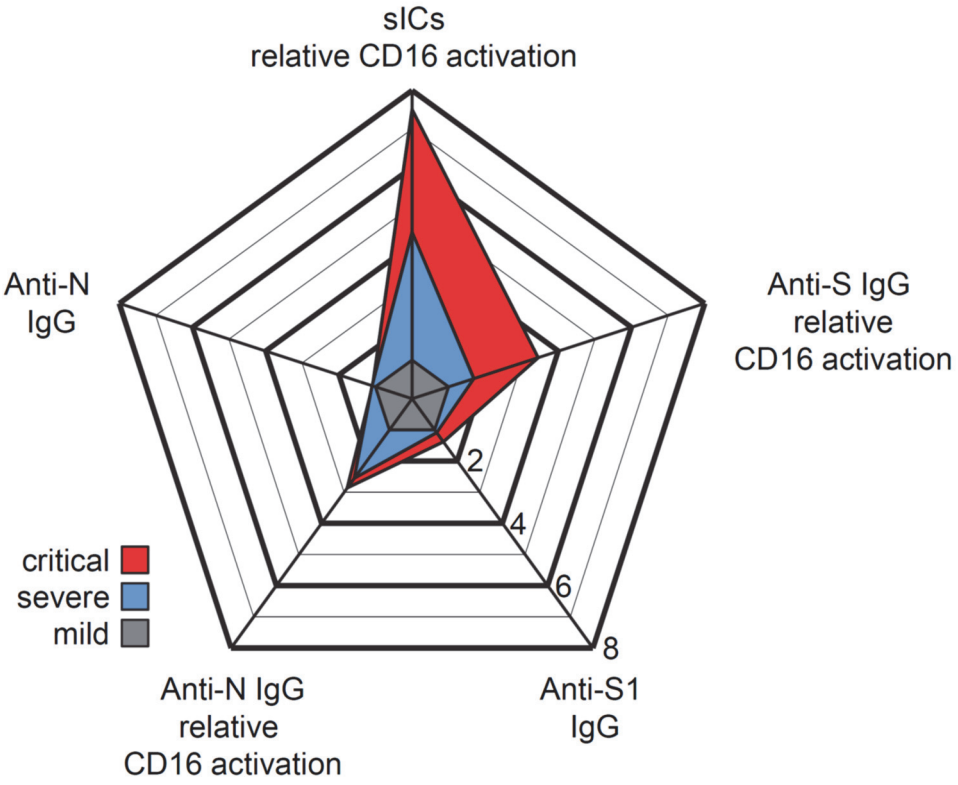

983

984